Since January 2020 Elsevier has created a COVID-19 resource centre with free information in English and Mandarin on the novel coronavirus COVID-19. The COVID-19 resource centre is hosted on Elsevier Connect, the company's public news and information website.

Colloids and Surfaces B: Biointerfaces 206 (2021) 111962

Contents lists available at ScienceDirect

Colloids and Surfaces B: Biointerfaces

journal homepage: www.elsevier.com/locate/colsurfb

Conventional and microfluidic methods for airborne virus isolation and detection

Sophie Krokhine [a], Hadis Torabi [b], Ali Doostmohammadi [c], Pouya Rezai [c,*]

[a] Faculty of Science, McMaster University, Burke Science Building, 1280 Main Street West, Hamilton, ON L8S 4K1, Canada
[b] Department of Biomedical Engineering, University of Isfahan, Iran
[c] Department of Mechanical Engineering, York University, ON, Canada

ARTICLE INFO

Keywords:
Virus
Airborne transmission
Virus collection
Virus detection
Microfluidics
Point-of-need

ABSTRACT

With the COVID-19 pandemic, the threat of infectious diseases to public health and safety has become much more apparent. Viral, bacterial and fungal diseases have led to the loss of millions of lives, especially in the developing world. Diseases caused by airborne viruses like SARS-CoV-2 are difficult to control, as these viruses are easily transmissible and can circulate in the air for hours. To contain outbreaks of viruses such as SARS-CoV-2 and institute targeted precautions, it is important to detect them in air and understand how they infect their targets. Point-of-care (PoC) diagnostics and point-of-need (PoN) detection methods are necessary to rapidly test patient and environmental samples, so precautions can immediately be applied. Traditional benchtop detection methods such as ELISA, PCR and culture are not suitable for PoC and PoN monitoring, because they can take hours to days and require specialized equipment. Microfluidic devices can be made at low cost to perform such assays rapidly and at the PoN. They can also be integrated with air- and liquid-based sampling technologies to capture and analyze viruses from air and body fluids. Here, conventional and microfluidic virus detection methods are reviewed and compared. The use of air sampling devices to capture and concentrate viruses is discussed first, followed by a review of analysis methods such as immunoassays, RT-PCR and isothermal amplification in conventional and microfluidic platforms. This review provides an overview of the capabilities of microfluidics in virus handling and detection, which will be useful to infectious disease researchers, biomedical engineers, and public health agencies.

1. Introduction

Throughout history, infectious diseases have posed a great threat to human health. This threat has become much more visible as the COVID-19 pandemic, caused by the SARS-CoV-2 virus, has swept the globe [1]. As of June 2021, over 170 million cases of the novel disease and 3.7 million deaths have been reported [2]. The SARS-CoV-2 virus is very transmissible, and although researchers have disagreed on whether it is airborne, it is known to be transmitted by respiratory droplets and contact with contaminated objects, known as fomites [1,3,4]. Airborne viruses are important to public health as they are responsible not only for COVID-19, but also for other infectious diseases such as influenza and measles [5,6].

Creating targeted and effective interventions to stop the spread of airborne infectious diseases requires a strong understanding of transmission modes, accurate air particle collection and sample preparation, and rapid, sensitive, and specific detection methods. Containing an infectious disease requires knowledge of pathogen circulation in the air in correlation with the distribution of infected cases. This knowledge can be acquired through Point-of-Care (PoC) diagnosis from body fluids or Point-of-Need (PoN) testing of indoor and outdoor air samples [7–10].

Currently used benchtop diagnostic methods including cell culture, polymerase chain reaction (PCR) and enzyme-linked immunosorbent assay (ELISA) require specialized equipment in centralized labs and can take 2–5 days to produce results, making them inappropriate for rapid and in-situ testing [11,12]. Using the benchtop versions of these tests can lead to underestimation of the true number of cases which can result in late and less effective intervention actions [11]. There are also few established methods for simultaneously capturing and analyzing viruses

* Corresponding author at: BRG 433B, 4700 Keele St, Toronto, ON M3J 1P3, Canada.
E-mail addresses: s.n.krokhine@gmail.com (S. Krokhine), hadis.torabi@yahoo.com (H. Torabi), doost@yorku.ca (A. Doostmohammadi), prezai@yorku.ca (P. Rezai).

https://doi.org/10.1016/j.colsurfb.2021.111962
Received 9 April 2021; Received in revised form 22 June 2021; Accepted 29 June 2021
Available online 2 July 2021

in the air, so it is difficult to know which regions have the highest rates of circulation and require stricter targeted precautions. Commercial air samplers such as the SKC BioSampler currently exist, but the additional amplification steps needed to detect and classify the particles can increase the time needed to generate results and reduce applicability in remote settings.

To solve these problems, researchers have turned to the field of microfluidics, which involves the flow of small volumes of single- and/or multi-phase fluids through microchannels and across micro-scale actuators and sensors [13–15]. Microfluidic chips are small enough to fit in a human hand and thus can be easily transported within resource-limited areas. Most microfluidic chips are made of plastic (polydimethylsiloxane-PDMS or polymethylmethacrylate-PMMA) or paper, so they are relatively inexpensive and mostly disposable and/or reusable. They can be used to carry out traditional bioanalysis techniques such as PCR and ELISA, or newer assays such as CRISPR-Cas and field effect transistor (FET) sensing, using much less time and reagent volumes than on a bench top. They can also be automatically operated and integrated with air samplers, making it possible to capture and analyze airborne particles in a single device with little to no user intervention.

This review focuses on the use of microfluidic techniques for airborne virus capturing and analysis. It includes three sections, focusing on (1) Mechanisms of Airborne Pathogen Spread, (2) Methods for Airborne Virus Collection and (3) Methods for Bioanalysis. In Section 2, airborne and zoonotic transmission methods are discussed. In Section 3, ways to collect viruses from the air are described and in section 4, conventional and microfluidic techniques for pathogen detection and typing are reviewed. It is important to note that some of the studies reviewed here used microfluidics for air sampling only, not analysis. Additionally, some studies in the bioanalysis section used different types of pathogens, like bacteria, and those that were not airborne. Nevertheless, these papers are included because we think their techniques could be useful for capturing and detecting viruses from the air. Compared to other recently published review papers [16–18], our review provides a more comprehensive account of the airborne virus detection process from start to finish, touching sequentially on airborne transmission, sampling and analysis methods. We discuss microfluidic applications of traditional techniques such as ELISA, PCR, and LAMP, as well as emerging techniques. We also discuss limitations and inconsistencies in previous works, such as the inconsistent use of units in limit of detection reporting. At the end of this paper, we provide our assessments of future trends in the field of microfluidics for virus detection.

2. Mechanisms of airborne pathogen spread

To monitor pathogens (including viruses) from the air and diagnose infections in patients, it is important to understand how they are spread. Viruses that spread through air, such as influenza and SARS-CoV-2, are the most easily transmissible. Transmission in air usually takes place in a four-step cycle (Fig. 1) involving 1) pathogen shedding by respiratory activities and formation of bioaerosols, 2) dispersion in the air, 3) infection of the recipient by inhalation or contact and 4) amplification of the pathogen within the host's body [19].

First, pathogens are assimilated into bioaerosols in the respiratory tract, which are created by respiratory activities such as breathing, talking, sneezing and coughing [20,21]. Bioaerosols are generally composed of one or more viruses along with mucus, salts and water and can range in size from several nanometers to several hundred micrometers [22,23]. After being released, they may either travel directly to the recipient or deposit on a surface and be re-aerosolized. The World Health Organization (WHO) classifies bioaerosols into two types, i.e., true aerosols (diameter of $\leq$5 μm) which can spread over distances greater than 1 m, and droplets (>5 μm) which can move over a shorter distances [23]. Aerosols tend to remain in the air longer than droplets

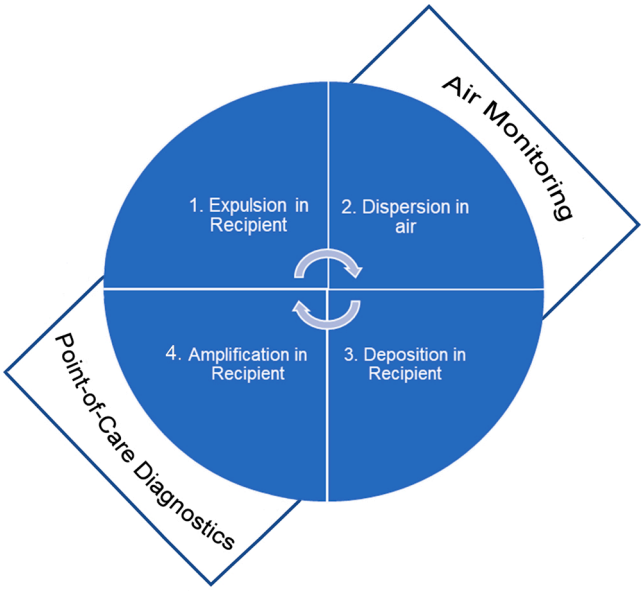

Fig. 1. Schematic of the pathogen transmission cycle, showing where sampling for air monitoring and PoC diagnostic techniques fit in.

and deposit in the lower respiratory tract, causing more severe clinical presentation [23,24]. Different precautions are recommended for each transmission route; while surgical face masks and gloves may protect against droplet and contact transmission, N95 respirators may be needed to keep out aerosols [5,25].

The 5 μm particle cutoff rule for aerosol classification does not take into account other factors such as viral load or environmental conditions which may influence deposition in the lungs. Nevertheless, it provides a starting point for classifying bioaerosols based on size. The size and number of bioaerosols generated depends on the type and frequency of respiratory activities performed [20,21,26]. For example, normal breathing usually produces aerosols from the upper respiratory tract, while talking, sneezing or coughing generates larger droplets from the movements of the vocal cords [6,19]. Aerosols can also be generated by healthcare procedures involving the lungs, such as ventilation, intubation and bronchoscopy [5]. The influence of different respiratory activities and environmental conditions on particle composition is reviewed in detail elsewhere [23]. Individual differences such as age also contribute to the variability in the number of particles exhaled, and "super-spreaders" (people who may exhale disproportionate amounts of particles and infect many others) contribute in large part to disease outbreaks [27,28].

After generation, the bioaerosols are dispersed in the air at low density. Bioaerosols usually absorb water from the mouth or respiratory tract, in a process known as hygroscopic growth [20]. Once they are released, the water may evaporate, thus reducing their size [23]. Relative humidity affects hygroscopic growth and evaporation, such that aerosols remain larger at higher humidity [20,23]. Viruses survive optimally at different temperatures and humidity levels. Enveloped viruses such as influenza and coronaviruses typically survive longer at lower temperature and humidity, while non-enveloped viruses such as rhinoviruses are more stable at higher humidity [29,30]. At low relative humidity, the salts inside aerosols and droplets may crystallize, which can protect viruses from degradation. The type of ventilation and air conditioning used indoors can also enable viruses to spread further and survive for longer, increasing the risk of transmission [5]. The effect of environmental factors on particle size is reviewed more comprehensively elsewhere [23].

Next, the pathogen deposits in the recipient, usually via inhalation or contact, and infects the respiratory tract. Bioaerosols can be inhaled directly from air containing them; they also often deposit on surfaces

such as walls, and objects including cellphones and door handles, as has been seen with COVID-19 [31–33]. Once a surface is touched, viruses can be re-aerosolized or introduced back into the air. A person's chance of becoming infected depends on the number of pathogens they are exposed to. The 50% human infectious dose (HID_{50}) is the dose corresponding to a 50% chance of infection in a susceptible individual [34]. HID_{50} is different for different viruses; for example, the HID_{50} for influenza virus is much greater than that for rhinovirus [34].

Finally, viruses are amplified or replicated in their new host, in either the respiratory tract or some secondary area. They can "hijack" cells' genetic machinery to replicate themselves through the lytic or lysogenic cycle [35,36]. In most cases, they will infect many of the cells in a given area, which sometimes but not always leads to symptoms. Viruses can also infiltrate immune cells to protect themselves from attack. Once viruses have been significantly amplified, they are shed through bioaerosols in the upper respiratory tract. Asymptomatic people can still shed the virus without knowing they have it, and can transmit it to their close contacts [6,37–39]. This is especially important for the spread of COVID-19.

Understanding the transmission cycle and specific transmission modes for each pathogen is important for planning appropriate precautions. Air monitoring focuses on identifying viruses at the second step, after they have been shed but before they have been deposited in the recipient. Disinfection, remediation and evacuation or quarantine measures can be applied to stop the transmission cycle there, and prevent many infections. Various methods for virus collection and detection in indoor and outdoor air samples are described in the following sections.

3. Methods of airborne virus collection

The majority of methods for virus analysis and detection require samples to be in a liquid or swab form, so aerosol and droplet particles must be collected and concentrated in a separate step. Several types of commercially available samplers can be used to do so, including impactors, cyclones, impingers, filters and electrostatic precipitators (Fig. 2 and Table 1) [40,41]. Selecting samplers for PoN testing or research requires understanding of their collection efficiency [42]. Two types of collection efficiency are measured, i.e., physical (the ratio of particles in the environment to particles captured by the sampler) and biological (the percentage of virus that stays viable after collection). Physical collection efficiency is usually measured by counting the numbers of particles entering and exiting the sampler, while biological collection efficiency is often measured by culture or plaque assay.

3.1. Impingers

The most commonly used sampling devices are liquid impingers, which work by forcing air containing viruses through nozzles into a collection medium (Fig. 2) [40,43]. The air flow rate differs from device to device [40,44]. The pressurized air forms bubbles on the surface of the collection medium, which can allow small particles to diffuse into the medium [41]. Most impingers are made of glass, although some can be made of metal [40,41]. The SKC BioSampler is a commercial glass impinger, which is used as a reference sampler in many of the studies described in this review [7,45]. It is designed to trap larger particles through impaction like a human respiratory tract, and it operates at a recommended flow rate of 12.5 L/min [41,45]. Impingers generally preserve viral infectivity, and their collection media can be directly harvested to perform an assay [27,46]. However, wall loss (adherence of virus to sampler wall preventing capture into the media), and re-aerosolization can be problematic, leading to lack of detection of positive samples and underestimation of the true concentration of viruses [44,47,48]. Evaporation of the impinger liquid may also take place at higher temperatures.

Impingers are often used to detect viruses such as SARS-CoV-2 because the liquid medium preserves viability [44]. Faridi et al. [49] used standard midget impingers at a flow rate of 1.5 L/min for sampling SARS-CoV-2 from 28 air samples in hospital wards and reported no virus detection using RT-PCR (PCR is discussed later). Ma et al. [27] used automated impingers to collect 26 air samples, along with surface swabs and exhaled breath condensates, in hospitals and COVID-19 isolation centers. Samples were analyzed with PCR, and a lower positivity rate was found for air samples (3.8%) than swabs (5.4%) and exhaled breath condensates (26.9%), possibly due to ventilation or inactivation by disinfectants. Kenarkoohi et al. [38] collected 14 air samples from different wards of a hospital, and two (in the ICU) were positive for SARS-CoV-2. These results mentioned above indicate that viruses were exhaled in a short time period, and further affirm the importance of bioaerosol transmission in the spread of COVID-19.

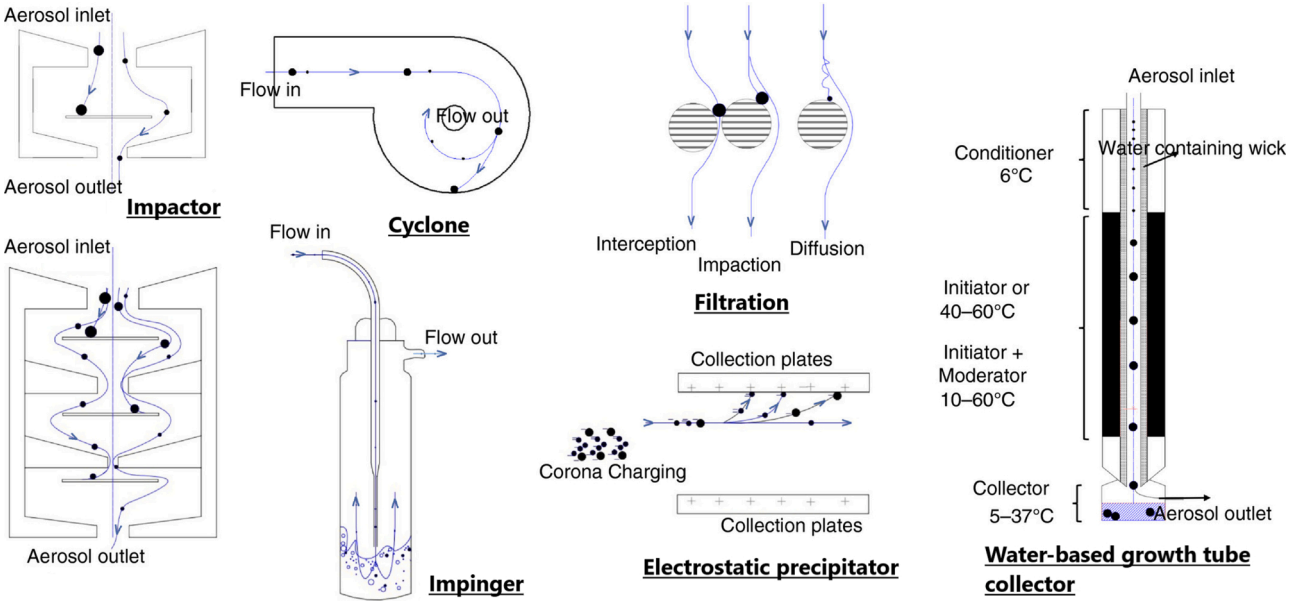

Fig. 2. Six main types of air samplers, i.e., impactors, cyclones, impingers, filters, electrostatic precipitators and water-based growth tube collectors. Reprinted from Pan et al. [40] with permission from the Journal of Applied Microbiology.

Table 1
Summary of advantages, disadvantages and uses of each sampling method.

Sampler Type	Description	Advantages	Disadvantages	References
Liquid Impinger	Captures virus particles through impingement onto a liquid medium. Example is the BioSampler.	Typically preserves virus viability, and the material can be directly used for assays without requiring additional extraction steps.	Wall loss and re-aerosolization are common.	Faridi et al. [49], Grinshpun et al. [47], Ma et al. [27], Mirzaee et al. [43], Springorum et al. [44] BioSampler used as reference in Cho et al. [52], Pardon et al. [7], Riemenschneider et al. [46], Kenarkoohi et al. [38]
Impactor	Uses principles of inertia for particles to impact onto solid collection media, often at different levels based on size (as in the Andersen Cascade Impactor).	Can separate virus particles based on size.	Wall loss is common, many particles are too small to impact on the media.	Andersen [50], Appert et al. [51], Hong et al. [48]
Cyclone	Particles impact onto spiral sampler wall or liquid medium due to centrifugal force.	Can produce highly concentrated samples.	Generally low collection efficiency for small particles (<10 μm). May cause structural damage to, and desiccation of, viruses.	Cho et al. [52], Lane et al. [33], Orsini et al. [53]
Filter	Particles are trapped by methods such as impaction, diffusion and interception. Can be made out of various materials including gelatin, cellulose, glass and metal nanofibers.	Can capture smaller particles with greater efficiency than other types of samplers.	Viruses are often inactivated through desiccation and extraction. Gelatin filters may preserve infectivity but are unstable under various environmental conditions.	Appert et al. [51], Kwon et al. [10], Mouchtouri et al. [31], Razzini et al. [32]
Electrostatic Precipitator (ESP)	Particles acquire charges through a corona discharge field, and are attracted to oppositely charged electrodes.	Can produce highly concentrated samples, and may require less power than other sampler types. Easily portable and, therefore, often integrated with microfluidic devices.	May damage viral infectivity.	Sandström et al.[54], Foat et al. [55], Pardon et al. [7], Tan et al. [8], Park et al. [9], Bhardwaj et al. [56]
Other Samplers	Other methods used, such as capturing viruses in water condensation tubes and causing them to impact upon the wall. May combine elements of other sampling methods.	Can preserve viral infectivity, and incorporate the benefits of multiple sampling techniques.	N/A	Damit [61], Hering and Stolsenberg [57, 58], Hering et al. [59], Novosselov et al. [60]

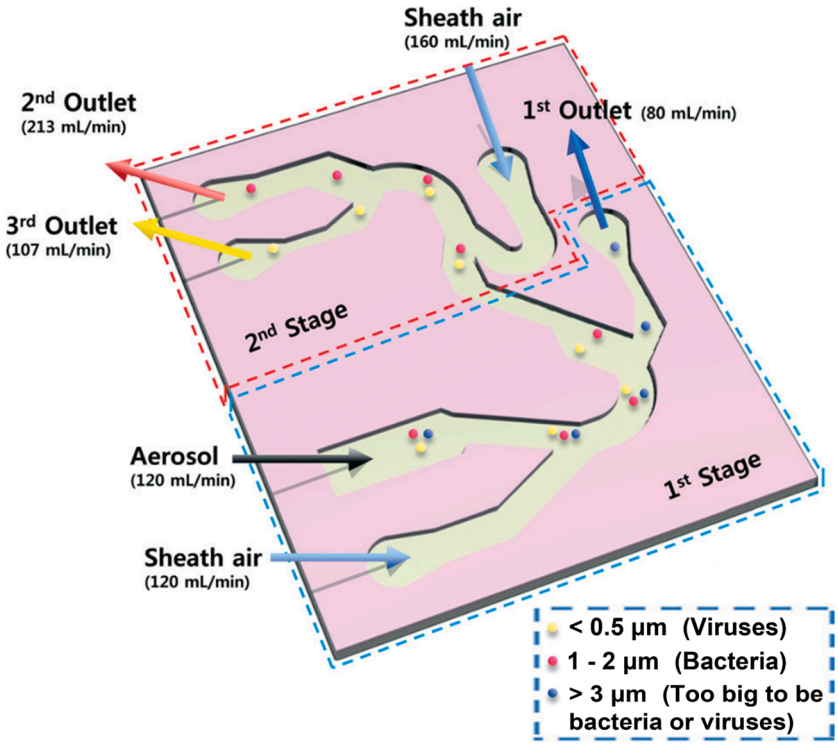

Fig. 3. Diagram of a curved channel inertial particle separator, with air inlets and outlets for particles inflow and outflow. Reprinted from Hong et al. [48] with permission from the Royal Society of Chemistry.

Mirzaee et al. [43] developed an impinger integrated directly on a microfluidic chip, which required significantly less time and reagent volumes than conventional impingers. The PDMS chip included intersecting gas and liquid channels, as well as gas and liquid inlets and outlets. Air containing 0.5, 1 and 2 µm polystyrene latex (PSL) particles was drawn into the chip by a vacuum pump operating at flow rates of 10−20 mL/min. Controlled bubbling at the ends of gas channels was used to trap small particles. Both mathematical modeling and experimental results indicated a physical collection efficiency around 90%.

3.2. Inertial samplers: impactors and cyclones

Impactors also involve air being drawn through a vacuum pump and pushed through nozzles, but onto solid surfaces rather than liquid collection media (Fig. 2) [48]. The deposition of particles onto surfaces is dependent on their inertia and mass, such that only particles within a certain size range may impact onto a specific surface [19]. The Andersen Cascade Impactor (ACI) separates particles by size using a series of six surfaces organized serially in the air flow direction; the largest particles impact on the first surface and particles of successively decreasing size deposit on the lower surfaces [9,50]. Unfortunately, some small virus-containing particles cannot impact on even the last surface and must be collected after by other methods such as filters [51]. Similar to impingers, impactors suffer the drawback of significant wall loss.

Hong et al. [48] developed an inertial size separator directly on a microfluidic chip. The chip had a main curved channel with 3 outlets designed to separate bacteria (*Staphylococcus epidermis*) from viruses (Adenovirus 40; Fig. 3). The outlets were positioned at 90° curves, and aerosols were pumped first at a flow rate of 120 mL/min to separate large particles (>3 µm) at the first outlet, then at 160 mL/min to separate bacteria-sized particles (1−2 µm) at the second outlet. Virus-size particles (<500 nm) exited at the third outlet. Gelatin filters were placed at each outlet to trap exiting particles for qPCR analysis. Results were acceptable with approximately 70% of 3.25 µm PSL particles exiting at the first outlet, 78% of bacteria exiting at the second outlet and 68% of viruses exiting at the third outlet. Bioaerosol losses were relatively low, i.e., 3.8% for viruses and 3.5% for bacteria. qPCR results confirmed that bacteria and viruses were efficiently separated.

Cyclones, also known as centrifugal samplers, are circular samplers that operate similar to impactors (Fig. 2) [33,52]. Centrifugal force disrupts the flow of air containing particles in cyclones, causing the particles to impact upon the collection wall. Cyclones are not very efficient for collecting low concentrations of virus particles; this may be why Lane et al. [33] found no positive SARS-CoV-2 air samples in a patient room using 2-stage NIOSH cyclones. Traditional cyclones may desiccate viruses, thus decreasing their infectivity, but “wet cyclones”, in which particles impact onto liquid media such as water, may provide gentler collection [52,53].

Cho et al. [52] created a device called the Automated and Real-Time Bioaerosol Sampler based on Wet-Cyclone (ARBSW) that was integrated with a microfluidic flow cytometer. The ARBSW consisted of a plastic funnel-shaped apparatus, with water forming a liquid film on the surface. The stark difference between the flow rates of the air, 16 L/min, and the liquid, 9 mL/hr, caused particles to quickly impact on the film and transfer to the flow cytometer. *S. epidermis* and *Micrococcus luteus* captured by the sampler were cultured, and the number of colony-forming units (CFUs) were counted. Sampling was carried out within 20 min, and the physical collection efficiency for bacteria was ~95%. Microbial recovery was similar to that of the reference BioSampler, suggesting that this technology should be explored more in the future.

3.3. Mechanical filters

It is often difficult to collect small particles with impingers or impactors, so filters provide an alternative [10,42]. Filters can be made of many different materials such as cellulose, glass fiber, mixed cellulose ester (MCE) and polytetrafluoroethylene (PTFE; Fig. 2). The mechanisms by which different types of filters remove particles are reviewed elsewhere [41]. Although convenient, filters tend to dry out viruses, and

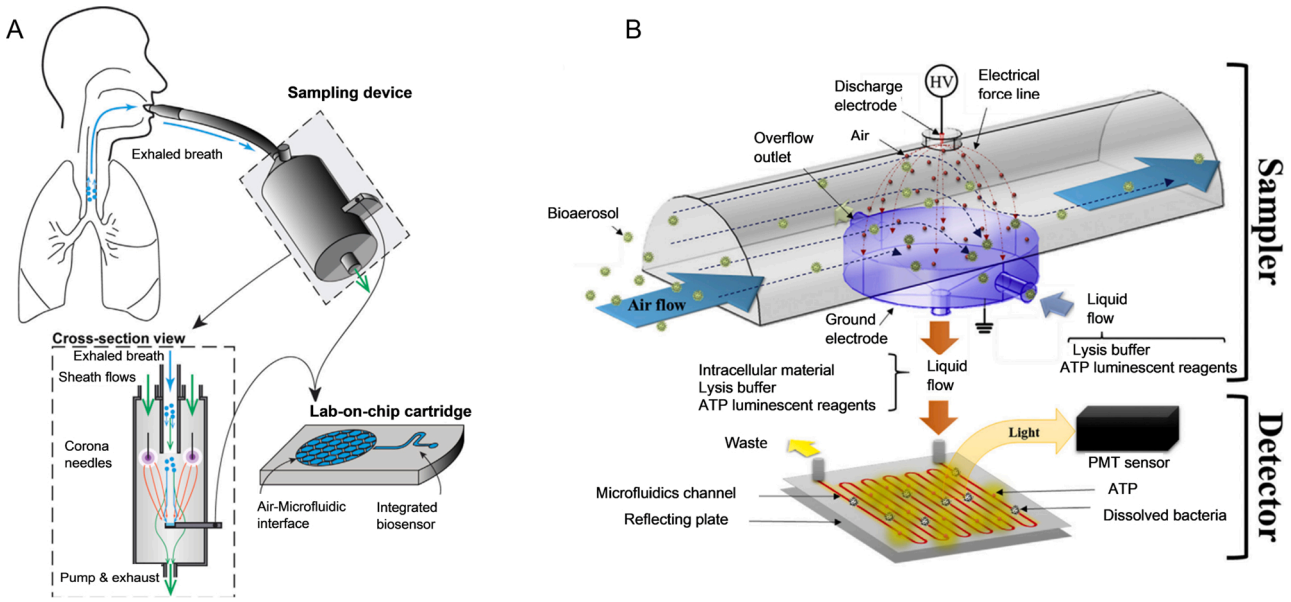

Fig. 4. A) Cross-sectional view of the exhaled breath condensate sampling device. Reprinted from Pardon et al. [7] with permission from Elsevier. B) The aerosol-to-hydrosol sampler and ATP bioluminescence detector.
Reprinted from Park et al. [9] with permission from Elsevier.

the process of extracting viruses can both damage their infectivity and eliminate the possibility of a direct sampling-to-analysis workflow. Gelatin filters can be dissolved in liquid post-capture and preserve viability; therefore, they are the preferred filter type for studies investigating infectivity [31]. Gelatin filters inside an MD8 Sartorius sampler have been used to detect SARS-CoV-2 from hospital air [31,32]. Mouchtouri et al. [31] tested 12 air samples in a hospital setting. One contained viral RNA; it was captured 2.5 m away from a patient not wearing a mask. Razzini et al. [32] also detected positive air samples in the ICU and corridor of a hospital. Nevertheless, because of the propensity of these filters to dry out or melt, they should be used for only short periods of time at moderate temperature and relative humidity [42,51].

3.4. *Electrostatic precipitators*

Another type of sampler that has recently become popular is the electrostatic precipitator (ESP), which uses electrostatic attraction to transport particles to a collection electrode (Figs. 2 and 4) [54,55]. Metal needles near the inlet of the ESP create a corona discharge which imparts charges on aerosols, so that they move towards the oppositely charged electrodes. Since ESPs carry less risk of damage to viruses than impactors or filters, create more concentrated samples, and are commercially available, they have commonly been integrated with microfluidic detectors [7,8]. However, the movement of particles by electric fields may cause damage to viral surface proteins and reduce infectivity, making certain assays more difficult to perform [56].

Sandström et al. [54] created a microfluidic electrohydrodynamic air pump (EHD) with an air-liquid interface for efficient transport and trapping of airborne particles. To transport particles directly to the air-liquid interface, the authors replaced the typical solid collector electrode with a liquid electrode. Similarly, Pardon et al. [7] developed a portable ESP system for capturing aerosols and droplets on a microfluidic air-liquid interface for analysis (Fig. 4A). Three corona discharge needles with an inter-electrode distance of 3 cm, as well as a liquid collector electrode, were used. The cylindrical sampler had two inlets to draw in particle and sheath flow, and one outlet which was connected to a BioSampler impinger. An aerosolized dye was used for testing, and particles that were not collected by the ESP were captured by the BioSampler. When the corona system was on, the ESP sampler demonstrated a collection efficiency of more than 20%. When the system was off, the collection efficiency remained below 1%, confirming that the use of the corona discharge greatly increased particle capture efficacy.

Tan et al. [8] designed an automatic electrostatic sampler (AES) for collection of pathogens from the air. The AES consisted of a semi-spherical steel electrode of diameter 6 or 16mm containing a central copper plate. Air was brought into the sampler at flow rates of 1.2 or 6.2 L/min and was passed through a particle charger consisting of two copper needles. Non-biological particles of 0.3−20 μm were used for testing the physical collection efficiency, and bacteria were sampled inside and outside to test the biological collection efficiency. For the 16 mm central electrode when the particle charger was applied, physical collection efficiency was higher at 1.2 L/min (above 90%) than at 6.2 L/min (60%). Fewer viable bacteria were collected indoors and outdoors by the AES than MCE filter, for both flow rates. The authors suggested that the AES could be integrated directly with an immunosensor for analysis.

Foat et al. [55] developed a personal ESP for pathogen detection, designed for the military. The 3D printed battery-powered sampler was operated at a flow rate of 5 L/min; air was drawn in through a small fan and passed through an inlet with corona needles. *Bacillus atrophaeus* spores, *Pseudonomas* bacteriophage 6 and sodium fluorescein particles were used in testing. A digital microfluidics (DMF) system based on electrowetting-on-diode (EWOD) was used to transport the sampled particles for analysis. In the EWOD process, particle-containing liquid from the sampler was formed into 2−3 μL droplets which were actuated across an electrode surface. These droplets were then used to perform reactions and assays. Collection efficiency for sodium fluorescein aerosols reached about 80%, but only for particles larger than 4 μm. Biological collection efficiency was quite low for *Bacillus atrophaeus* spores (2.7%). Follow-up tests determined this may have been due to corona discharge damaging the hydrophobicity of the actuation surface, which should be solvable.

In the study by Park et al. [9] a single-stage electrostatic precipitator, called an “aerosol-to-hydrosol” sampler, was used to capture airborne *S. epidermis* (Fig. 4B). The aerosol-to-hydrosol sampler was composed of a polycarbonate sheath with a liquid sampling well inside, and it operated at a flow rate of 8 L/min with an applied voltage of −7 kV. Aerosols

Table 2
Summary of main analysis techniques, advantages and disadvantages.

Analysis Technique	Description	Advantages	Disadvantages	References
ELISA	Specific antibodies conjugated with a substrate are bound to the antigen. The substrate is modified by an enzyme, creating a colorimetric change. Depending on the type of ELISA, secondary antibodies may be needed.	A well-established technique which has been used in virus detection for many years. Highly sensitive and specific, and can be integrated with microfluidic chips.	Conventional ELISA can take over 12 h. Difficult to produce antibodies, usually requiring animals such as mice. ELISA may not work well for all virus types.	Coarsey et al, [68], Dimov et al. [64], Y. Liu et al. [63], Yanagisawa and Dutta [65], Yeh et al. [86], Nicol et al. [74], Lu et al. [67]
SPR	Light is beamed at a sensor covered by metal film, and the intensity of refracted light is measured. Intensity is lowest at a specific refraction angle, and binding of analytes to receptors on the sensor surface changes this angle.	Label-free, which allows for the collection of direct information about pathogen binding and concentration. Can determine concentration of analyte and acquire data about biological reaction kinetics. It is a highly sensitive technique with low LOD.	Sensors can be difficult to reuse, as analyte or nonspecifically bound components may be left over after sensor washing, and the regeneration process may damage ligands.	Chang et al. [70], Huang et al. [73], Usachev et al. [71]
LFIA	Liquid sample is placed on a strip made of a porous material. It flows downstream to interact with dried conjugate. If the target analyte is present, it will form a test line.	Technology is well-established. Rapid, usually generating results within minutes. Inexpensive to produce and distribute.	Relatively low sensitivity. Typically, only provides a "yes-or-no" answer without quantitative results.	Nicol et al. [74], Rong et al. [79], Wu et al. [77], Xiang et al. [78], C. Wang et al. [108]
PCR	Nucleic acid is replicated with the addition of primers. Thermal cycling takes place in stages, usually between about 30 and 95 °C.	Commercially used technology which can be integrated with microfluidic chips. High sensitivity and specificity with low limit of detection. Amenable to multiplexing.	Conventional PCR takes hours and requires specialized lab equipment. Achieving the desired thermal cycling can be hard on a microfluidic chip.	Ma et al. [27], Lane et al. [33], Razzini et al. [32], Faridi et al. [49], Foat et al. [55], Yeh et al. [86], Prakash et al. [85], Huijskens et al. [82], Olive et al. [83], Farshidfar et al. [84]
LAMP	Nucleic acids amplified, using 2–3 sets of primers, at a constant temperature (usually about 60–65 °C)	Low cost, ease of use, does not require thermal cycling, relatively low LOD.	Relatively low specificity (high false positive rate), due to the concentrations of primers used.	Coelho et al. [93], Fujino et al. [89], Ganguli et al. [95], Q. Liu et al. [90–92], Y. Liu et al. [88], Rodriguez-Manzano et al. [96], Sun et al. [94], R. Wang et al. [12], Xiong et al. [98], Tian et al. [97]
Microscopy	Virus particles viewed and counted with a microscopy apparatus, often using fluorescence.	Some microscopes can be integrated directly with a smartphone, detection is usually very rapid.	Viruses can be difficult to count visually due to agglomeration and background noise.	Ming et al. [104], Ray et al. [102,101], Wei et al. [103]
Other Techniques	Includes immunoassays such as chemiluminescence immunoassay (CLIA), Mie scattering analysis, field-effect transistor (FET) sensing, surface-enhanced Raman spectroscopy (SERS) and CRISPR-Cas.	Dependent on the technique. CLIA and FET are both quite rapid with high sensitivity. Scattering analysis can be done with a smartphone. CRISPR-Cas is very rapid.	Dependent on the technique. If labeling involved, throughput may be impaired. FET may have cross-reactivity. SERS requires special substrates.	CLIA: reviewed in Zhao et al. [75], used in Nicol et al. [74]. FET: Seo et al. [113,114], Uhm et al. [109]. Mie scattering with immunoassay: Kwon et al. [10]. SERS: H. Liu et al. [107], Kukushkin et al. [105], H. Chen et al. [106], C. Wang et al. [108] and Shen et al. [81,110], Qin et al. [115], Mayuramart et al. [116]

passed through the sampling well into a stainless-steel ground electrode, where they were captured in a flow of liquid-containing lysis buffer and fluorescent reagents.

3.5. Other samplers

Various other sampling devices have been used for airborne viruses. One example is the water-based growth tube collector, in which aerosols are placed in a tube surrounded by cooled water [57–59]. Water vapor in the tube condenses, capturing the particles in larger droplets which impact onto the wall of the tube. This can be used to quantify bioaerosols in condensation particle counters (CPCs) [58]. Some researchers have created "custom samplers" that combine several of the above techniques [60,61]. Novosselov et al. [60] used a W-shaped microchannel collector (μCC), in which particles impacted onto the wall by centrifugal force. The collection efficiency was about 50% for 0.5 μm PSL particles and close to 100% for 2 μm particles, and the authors suggested that such a collector could be integrated into microfluidic systems. Damit [61] successfully distinguished aerosols containing dead *E. coli* from non-biological aerosols using a droplet-based microfluidic platform. Droplets containing the fluorescence agent propidium iodide were created at the intersection of fluid and oil channels. Both types of aerosols were sprayed from above and absorbed onto the surface of droplets. The droplets containing *E. coli* were selectively stained and had a bulk fluorescence measurement about 20–30 times greater than those containing non-biological particles.

4. Methods for bioanalysis

Once viruses have been captured in sampling, multiple methods are commonly used to detect and analyze them. Such methods include immunoassays, involving detection of specific antigens or antibodies, nucleic acid amplification, involving copying and detection of specific regions of a viral genome, and visualization via microscopy. In this section, we will describe these methods in the context of conventional assays as well as their implementation or integration into microfluidic devices. These methods, and their applications to microfluidics, are also summarized in Table 2.

4.1. Immunoassay based detection

Many biosensors have used the natural properties of the immune system, involving antigen-antibody interactions to detect and quantify pathogens. Examples of immunosensing techniques that are described below include enzyme-linked immunosorbent assay (ELISA), surface plasmon resonance (SPR) and lateral flow immunoassay (LFIA).

ELISA is commonly used for detecting pathogens including viruses. It operates on the principle of specific antigen-antibody binding, i.e. antibodies bind to a certain region (epitope) of an antigen, and each antibody only recognizes one or a group of antigens [62]. Conventional (benchtop) ELISA can take several hours, too long to quickly catch the spread of disease [63].

Microfluidic devices have been used to perform ELISA in real-time, as in the study by Dimov et al. [64]. A DMF platform based on EWOD was introduced to perform automated ELISA on four different targets; although the samples were not airborne, one of the targets was the MS2 bacteriophage. ELISA was performed using MS2-specific antibodies immobilized on magnetic beads. Minimal volumes of reagents were used, and the entire assay could be completed in 6−10 min. Y. Liu et al. [63] used reciprocating-flow ELISA on a microfluidic chip for detection of SARS-CoV-2 antibodies from the serum of 13 patients within 5 min. Pressure was exerted and removed from the fluid, allowing it to flow back and forth and improving binding to immobilized antigens. The device achieved 100% sensitivity and specificity and a LOD of 4.14 pg/mL.

In another microfluidic device developed by Yanagisawa and Dutta [65], kinetic ELISA was used to detect blue tongue virus (BTV) and epizootic hemorrhagic disease virus (EHDV) antibodies, which were extracted from the body fluids of mice and rabbits. Capture antibodies were first immobilized onto a glass microchip with etched channels, and the chip was then incubated in solutions of BTV and EHDV antibodies. In kinetic ELISA, fluorescence was measured 6–7 times during the reaction period, nearly in real-time. It linearly increased with time, showing the progression of the reaction. Kinetic ELISA was also performed on a commercial microwell plate for comparison. The microfluidic platform showed significantly better performance than the microwell plate, with a 3x lower limit of detection (LOD).

While ELISA is commercially available, even on a microfluidic chip it is not always suited for rapid PoC and PoN diagnosis. Before performing ELISA, researchers must have antibody solutions (antisera) available [62]. The long and costly process of creating antisera involves immunizing animals, often mice, against a pathogen multiple times before isolating antibodies from the animals' blood [62,66]. Additionally, ELISA may not work well for detecting all types of viruses [66].

Overall, many techniques were found to be useful for detection of viruses from air [16–18]. However, the effectiveness of various analysis devices and techniques is difficult to compare because the sensitivity, specificity and LOD are measured differently across studies. LOD is measured in different units: e.g., copies per reaction, copies per mL, pg per mL, plaque-forming units (PFU), and colony-forming units (CFU). Additionally, cut-offs for determining positive results and distinguishing virus presence from background signals differ across studies. The use of a standard unit of LOD and signal threshold would make it easier to report results and detect viruses.

Immunoagglutination, which involves the detection of clumps of magnetic beads conjugated to antibodies, is a technique used to carry out immunoassays such as ELISA. Immunoagglutination has been used for detection of viruses including influenza [10,67], and is often used in combination with a DMF platform as in the studies by Coarsey et al. [68] and Lu et al. [67]. The latter used magnetic beads conjugated to H1N1 aptamers for detection of H1N1 virus by ELISA-like assay. Each droplet on the surface functioned as a "micro-reactor", and droplet motion was controlled with an Arduino. Detection could be completed within 40 min, with a LOD of 0.032 hemagglutination units (HAU).

The SPR immunosensor was first commercialized in the 1990s as an alternative to ELISA [69]. In an SPR apparatus, light is beamed at a sensor covered by metal film at a specific angle, and the intensity of light being reflected is measured. Of interest is the angle at which surface plasmons are excited and the lowest refraction intensity is achieved, known as the resonance angle or "SPR-dip". The resonance angle is affected by the refractive indices of metal on both sides of the sensor. When introduced antigens bind to ligands on the sensor surface, they change the refractive index on one side, causing a change in the resonance angle and enabling detection of the pathogen. A regeneration solution is then added to wash off bound antigens and allow the sensor to be reused, although ligands or metal coating may also be washed off in this step, reducing the efficacy of the sensor. Detection is label-free, meaning that no enzymes or other conjugates are needed [70].

Usachev et al. [71] used a microfluidic SPR sensor coupled with an air sampler for real-time detection of MS2 aerosols. Once aerosols were generated by a nebulizer, they were captured by a 'bubbler' air sampler similar to that used by Agranovski et al. [72]. Sampling times were 1, 5 and 25 min and the flow rate used was 4 L/min. MS2 could be qualitatively detected after 2 min, and the entire detection and analysis process was completed within 6 min. The sensor was specific to MS2, exhibiting no cross-reactivity with influenza A viruses or m13 and T4 phages. It was also shown to be durable, exhibiting a relatively small decrease in performance of 30% after 5 weeks of continuous use. Similarly, Huang et al. [73] used a nano-SPR sensor for detection of SARS-CoV-2. Non-infective SARS-CoV-2 pseudoviruses created by genetic engineering were bound to antibodies immobilized onto the surface of the nanosensor. Gold conjugated angiotensin-converting enzyme

(ACE) proteins were then attached to the spike proteins of these pseudoviruses, facilitating detection. The nanosensor was integrated into both a standard 96-well plate and a handheld cartridge linked to a smartphone app. Results were generated within 15 min and no cross-reactivity was observed for SARS, MERS and vesicular stomatitis virus (VSV). The LOD was reported to be considerably higher for the handheld device than the 96 well plate (4000 copies per reaction as opposed to 30).

Many variations of immunoassays that do not fit into the above categories have been used. Several studies using these non-standard immunoassays are reviewed below.

Chemiluminescence assays (CLIs) involve a chemical reaction between antibodies or antibody fragments and specific labels, generating luminescence. Labels include luminol, actinidium ester and metal-conjugated magnetic particles, and enzymes may catalyze the light-producing reactions [74]. The general methodology and advantages of CLI are reviewed elsewhere [74,75].

A final class of immunoassays commonly used for PoC diagnostics from body fluids are lateral flow immunoassays (LFIAs, [76]). These tests are exceptionally rapid, delivering results in about 10 min, and are easy to manufacture and mass-produce. Because they come in the form of small strips, they are also portable and can be distributed to low-resource locations. In SARS-CoV-2 detection, antibody tests by LFIA are used to identify those who have been previously infected or to diagnose those who are negative by RT-PCR [74]. IgG, IgM and/or IgA are usually detected from whole blood, serum or plasma within 10−15 min. Nicol et al. [74] used ELISA, CLIA and LFIA to detect SARS-Cov2 IgM, IgA and IgG antibodies. Sensitivity for all three methods and all three antibody types was below 60% in the first 7 days after symptom onset and reached 100% 14 days after symptom onset. Specificity for IgG was lower for ELISA (96.7%) than CLIA (99.3%) and LFIA (98%). In another study, the sensitivity to SARS-CoV-2 IgG antibodies reached 100% after 21 days [77]. Perfect specificity was observed in all time intervals after symptom onset. LFIAs have also been used to detect other human viruses such as Hepatitis C and Zika from serum, with high specificity and sensitivity, and they could be used to analyze concentrated samples collected from air [78,79]. Xiang et al. [78] used a double-antigen sandwich (DAS) LFIA to detect hepatitis C virus (HCV). The assay's sensitivity and specificity, measured using 23 positive and 8 negative HCV samples, were each 100%. When 300 samples were tested with both DAS-LFIA and ELISA, 94% concordance was observed. Unfortunately, LFIAs tend to have lower sensitivity than molecular methods such as PCR and it is difficult to gather quantitative information from their visual format [76]. Air monitoring should use primarily quantitative detection methods, because knowing the amount of virus present in an area is important for determining the extent of community spread.

4.2. Nucleic acid based detection

4.2.1. Polymerase chain reaction (PCR)

In addition to antibody- and antigen-based assays, nucleic acid amplification is used to detect pathogens. PCR has been one of the most commonly used lab techniques since its inception in the 1980s, as reviewed before [80]. PCR can create millions of copies of target DNA or RNA regions for later quantification with gel electrophoresis.

Conventional PCR is a long process that can take hours to complete, but quantitative PCR (qPCR) can detect products in real time and significantly speed up diagnosis [81–83]. Currently, qPCR is the 'gold standard' for COVID-19 diagnosis, but the risk of healthcare worker infection from collecting samples has necessitated alternative diagnostic methods [27,31–33,49,84]. It has also been used to detect various human viruses including rhinovirus, respiratory syncytial virus and cytomegalovirus [82,83]. For example, Huijskens et al. [82] used PCR to detect 19 respiratory viruses and *Mycoplasma pneumoniae* in the nasal secretions of 177 children, in a retrospective study. 73% of children had at least one virus, mainly RSV (37%) and Human Rhinovirus (24%). Those with a respiratory pathogen were more likely to be hospitalized and present with symptoms like rhinorrhea and dyspnea.

Conventional PCR is not sufficient for rapid diagnosis in resource-poor areas because it is expensive and requires a skilled user and a centralized laboratory [80]. However, performing PCR on microfluidic chips may provide a way to overcome these limitations. For example, Prakash et al. [85] used a multiplex reverse-transcription PCR (RT-PCR) technique for detection of Influenza A and B viruses from clinical samples. Their microfluidic device consisted of two chromium heater blocks attached to a glass chip, creating different temperature zones. Reaction microdroplets moved between these zones by droplet-dielectrophoresis (D-DEP), in which droplets were actuated across herringbone electrodes.

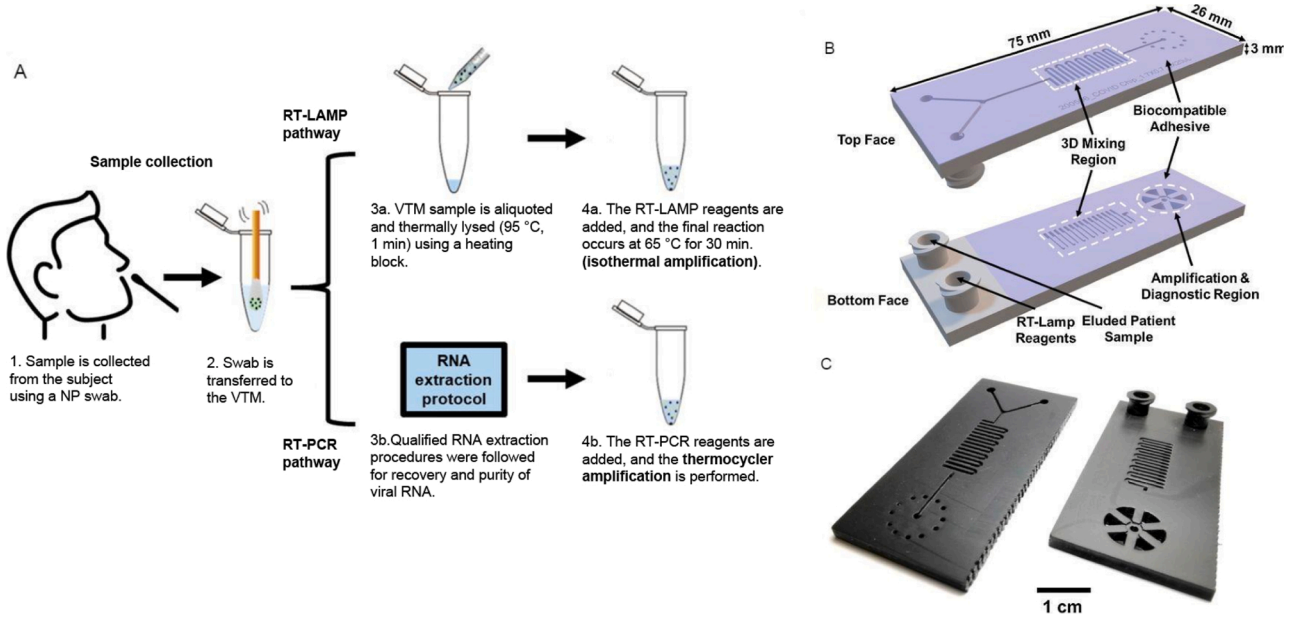

Fig. 5. A) Schematic of LAMP versus PCR SARS-CoV-2 detection pathway from nasopharyngeal swab. B) Schematic of the LAMP detection chip. C) Photograph of LAMP detection chip.
Reprinted from Ganguli et al. [95] under Creative Commons Attribution License 4.0 https://creativecommons.org/licenses/by/4.0/.

Eight reactions could be carried out in parallel, enabling both spectral (multiple analyses on the same droplet) and spatial (multiple samples in parallel) multiplexing. A fluorescent dye conjugated to the PCR products effectively signaled the presence or absence of these viruses. Known positive and negative influenza samples were first used, followed by "blind panels" of influenza A (FluA) and mixed influenza A/influenza B (FluB) positive and negative samples. All positive and negative FluA and FluB samples were correctly detected from the blind panel, indicating 100% sensitivity and specificity. Olive et al. [83] performed a PCR assay for human cytomegalovirus (HCMV) detection in 24 clinical isolates and the urine of 6 renal transplant patients, with 100% sensitivity and 100% specificity (no reaction to other herpesviruses).

Yeh et al. [86] developed a carbon nanotube size-tunable enrichment microdevice (CNT-STEM) for concentrating and filtering virus samples, enabling PCR detection at concentrations well below the usual LOD. The device consisted of nitrogen-doped multiwalled carbon nanotubes (N-MWCNTs) created from iron catalyst thin films within a PDMS chamber. Virus-containing solutions were flown through the device, and viruses were trapped between the nanotubes while smaller contaminants passed through the spaces in between. Three types of analyses were done, i.e., immunofluorescence, RT-PCR, and virus isolation (to confirm viability). The chip was also integrated with next-generation sequencing (NGS) to identify a novel virus in turkeys. Once the virus was captured and sequenced, it was found to be a type of infectious bursal disease virus.

4.2.2. Loop-mediated isothermal amplification (LAMP)

Isothermal amplification, in which nucleic acid segments are amplified at a constant temperature, is an alternative to PCR which does not require the same cost and specialized equipment. The most commonly used amplification technique is LAMP, which is discussed below.

In LAMP, forward and backward primers are used to create looped segments of DNA which can then be detected by fluorescence or other methods [87]. LAMP is conducted at a constant temperature of 60−65 °C and generally takes 100 min or less to complete [12,88–94]. LAMP has been widely integrated with microfluidic chips for pathogen detection due to its low LOD, low cost, and ease of use. It has been performed on microfluidic chips for SARS-CoV-2 detection, with test results generated in 20−70 min ([94–97]; Fig. 5). In each of these studies, the presence of the virus was detected by fluorescence, which was analyzed by lab instruments or smartphones. The LODs for on-chip LAMP ranged from 2 to 50 copies per μL reaction. Ganguli et al. [95] correctly detected 5 positive and 5 negative SARS-CoV-2 samples on their cartridge instrument and 10 positive and 10 negative samples on the benchtop, indicating 100% sensitivity and specificity. Rodriguez-Manzano et al. [96] achieved slightly lower sensitivity (91%) and 100% specificity in 127 positive and 56 negative samples. Xiong et al. [98] used a microfluidic disk for multiplex detection of 7 human coronaviruses (SARS-CoV, SARS-CoV-2, HCoV-229E, HCoV-OC43, HCoV-NL63 and HCoV-HKU1) from clinical samples. Samples were centrifuged, and LAMP was completed within 40 min. 100% sensitivity and specificity, and 100% agreement with RT-PCR, were observed. Only liquid and nose swab samples were used in these coronavirus studies, but such systems could be integrated with samplers for air monitoring as well. R. Wang et al. [12] performed multiplex detection of Influenza A subtypes H1N1, H3N2, H5N1 and H7N9, Influenza B and human adenovirus in 109 clinical samples. 96% sensitivity and 100% specificity were achieved.

Q. Liu et al. [90] reported a microfluidic system for rapid direct detection of airborne *Pseudonomas aeruginosa* bacteria. A portable system was constructed containing a microfluidic chip along with a central circuit board, heater and detection modules. Air containing bacteria was vacuum-pumped onto the chip, passing through enrichment channels before reaching the LAMP detection chamber. LAMP products were illuminated by a fluorescent dye, SYBR green 1 [99], to enable detection. Results were viewed on an LCD screen integrated into a box, and the bacteria was reliably detected within 70 min. In a later study, the same authors detected *Staphylococcus aureus*, *Klebsiella pneumonia*, *Acinetobacter baumanii and P. aeruginosa* from the air using disposable microfluidic chips [91]. Detection was semi-quantitative, and standard quantity-time curves were generated for each species of bacteria. LODs of 50 or fewer copies in a 6.6 μL reaction volume were observed for each species.

In a third study [92], a semi-porous membrane (microfilter) was integrated onto microfluidic chips for pathogen concentration and enrichment. Airborne *P. aeruginosa* was detected as in the previous study, with an observed collection efficiency above 99%.

4.3. Microscopy-based detection

Another technique for detection of viruses, and other nanoparticles and micro-organisms, is to visualize them directly using microscopy. Many microscopes, such as electron microscopes, are sensitive enough to allow viewers to see nanoparticles and viruses [100]. Because many of these sensitive microscopes are expensive and require a trained user, lens-free holographic microscopy and smartphone attachments have also been developed.

Holographic microscopy works by illuminating a sample (which can be liquid, in a disposable microfluidic device) from below and then digitally reconstructing the diffraction pattern into an image, or

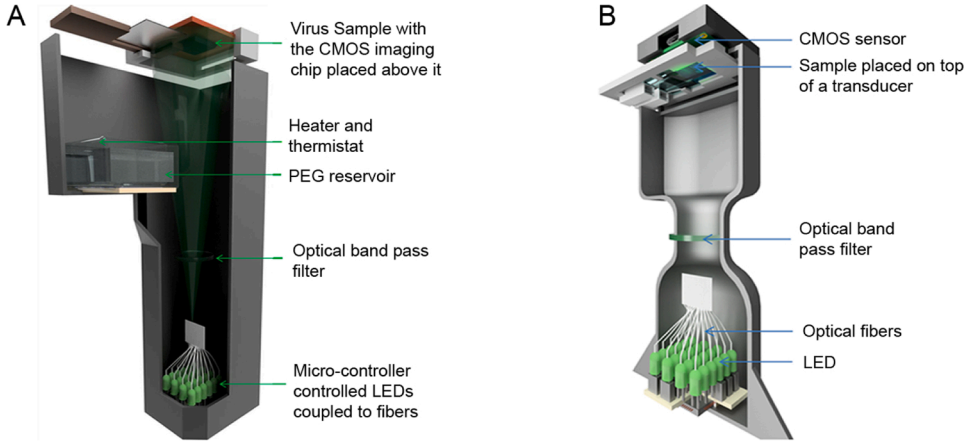

Fig. 6. A) and B) Schematics of holographic microscopes showing different parts of the apparatus.
Reprinted from Ray et al. [101], and Ray et al. [102] respectively, both with Creative Commons Attributions 4.0 International License, http://creativecommons.org/licenses/by/4.0/.

hologram. These microscopes are portable and often do not include lenses, but nanolenses may form when a Lamb-type wave reshapes the fluid on the substrate, making particles easier to view as shown in Fig. 6 [101,102]. Ray et al. [101] used a holographic microscope for counting and estimating the concentration of herpes simplex virus. Virus particles were conjugated to magnetic beads and then attached to antibodies on a glass surface. The recovery rate was lower than expected due to possible virus disintegration, difficulty with separating viruses which were close together and the contributions of background signals in the field of view.

Microscopy can also be performed with apparatuses attached to a smartphone, to reduce cost and increase portability. In the study by Wei et al. [103], a smartphone-integrated apparatus was used for detection of fluorescently labeled human cytomegalovirus (HCMV) particles. It consisted of a laser excitation diode, an interference-based filter, an external lens, and a focusing stage. Aggregated virus particles were associated with greater fluorescence intensity than single ones, and the density of viral particles measured with the microscope was strongly correlated with initial viral concentration. Ming et al. [104] used a quantum barcoding system for multiplex detection of various viruses. Polystyrene nanoparticles infused with quantum dots acted as barcodes for each virus, and had specific probe molecules which recognized and bound to viral genetic material. The barcoded beads created different colors of fluorescence after laser excitation. Multiple emission filters were used to reduce background noise and distinguish viruses. Images were taken by an iPhone camera, and an analysis algorithm was used to determine the presence of viruses. HIV, hepatitis B virus (HBV), HCV, influenza A H1N1, H5N2 and H3N1 and influenza B viruses were successfully detected, and HIV and HBV clinical samples were detected with 100% sensitivity and specificity and a LOD below 1000 copies/mL. While these studies only analyzed virus samples from liquid or cell culture, we believe that both holographic and smartphone-based microscopy could be used to analyze the liquid collected from air samplers.

4.4. Recent analytical virus detection techniques

Over the past few years, research in virus detection and diagnosis has expanded and advanced biosensing techniques have fallen into widespread use. Such techniques can be used to replace, or to complement, more conventional techniques discussed earlier in this review.

Surface-enhanced Raman spectroscopy (SERS) is the use of a special substrate with Raman spectroscopy to greatly amplify the Raman signal via the SPR effect. It can either be used on its own or to enhance the sensitivity of LFIA. SERS has been used to create aptamer-based sensors for influenza virus [105,106]. In the study by Kukushkin et al. [105], a sandwich assay was used in which primary aptamers were bound to both the surface and the virus and secondary aptamers were bound on top. Various strains of influenza A were detected, including H1N1, H3N2, H5N1, H5N3, H7N9 and H12N2. The LOD for H3N2 was 10^{-4} HAU, meaning the device's sensitivity was above that of LFIA but below that of PCR. H. Liu et al. [107] developed an LFIA using silver-coated SiO_2 nanoparticles (SiO2@Ag NPs) instead of the usual colloidal gold particles for more sensitive detection of SARS-CoV-2 antibodies. Out of 49 negative and 19 positive samples, all negatives and all but two positives were correctly identified. C. Wang et al. [108] created a multiplex LFIA for detection of H1N1 influenza virus and human adenovirus with silver-coated Fe_3O_4(Fe3O4@Ag) magnetic nanoparticles as SERS tags. The system achieved a LOD of 50 PFU/mL for H1N1 and 10 PFU/mL for adenovirus.

Field effect transistor (FET) based sensing is also a promising method for virus detection and analysis [81,109–111]. In FET, surfaces are modified by the addition of receptors or ligands to which target analytes bind, inducing a conductance change which is measured. FET can be done with carbon nanotubes, silicon nanowires (SiNW) or graphene as reviewed in [112]. Seo et al. [113,114] used a graphene based FET for detection of SARS-CoV-2, with a LOD of 1 fg/mL. Uhm et al. [109] used SiNW sensors fabricated by a complementary metal oxide semiconductor (CMOS)-compatible process to detect the hemagglutinin HA1 surface protein of influenza virus. CMP-NANA probes were immobilized on the SiNW surface and bound to HA1, which was detected at concentrations as low as 1 femtomolar. Earlier, Shen et al. [81] used a SiNW-FET system for detecting airborne influenza A H3N2 and H1N1 viruses. Viruses were collected with the automatic electrostatic sampler used by Tan et al. [8]. The liquid was then pipetted or drawn onto a microfluidic chip containing silicon nanowires conjugated to H3N2 antibodies. A significant conductance change was observed in air samples containing the virus within 1−2 min, and the LOD was below 10^4 copies/L. However, none of the virus-containing air samples could be detected by qPCR in this study. In 2012, the SiNW-FET sensing method was used for diagnosing influenza from exhaled breath condensate (EBC) [110]. EBC of patients with and without clinical flu symptoms was tested; positive swab samples were generated by spiking EBC of patients without flu and liquid from indoor air samples with H3N2. The SiNW system could reliably detect the viruses in most cases, although an unusually high conductance response was observed for an H1N1 sample, possibly indicating cross-reactivity. As with SPR, the SiNW system faces the drawback of antibodies falling off after time or viruses remaining bound to the surface, limiting the test's effectiveness.

CRISPR-Cas is another innovative tool assisting with detection of viruses. Cas12 and Cas13 nonspecifically cleave DNA and RNA respectively, leading to the cleaving of a fluorescence reporter when viral genetic material is present. Qin et al. [115] used CRISPR-Cas13 on a microfluidic chip for detection of Ebola virus. Similarly, Mayuramart et al. [116] used CRISPR-Cas12 for detection of SARS-CoV-2 and Influenza A and B, with LODs below 1000 copies/reaction.

5. Summary and conclusions

Microfluidic devices are well suited for monitoring the spread of infectious viruses in the air and provide rapid diagnosis, the importance of which has been highlighted during the COVID-19 pandemic. These devices are portable, low-cost and can carry out reactions very quickly. Many advances have been made in sampling viruses directly from the air and concentrating these samples for downstream analysis. On-chip, a wide variety of analysis techniques such as immunoassays, RT-PCR and LAMP have been used which have enabled detection within minutes. This has included novel COVID-19 tests; however, few commercially available methods for SARS-CoV-2 detection from air currently exist.

Usually, air sampling is done before analysis. Therefore, this review focused on both sampling and macro- to micro-fluidic analysis techniques. We reviewed several sampler types including liquid impingers, impactors, cyclones, and electrostatic precipitators. In some cases, samplers were integrated directly with microfluidic devices, although this was rare. While samplers could generally produce concentrated samples for direct analysis, most damaged or inactivated viruses, which could render them less useful for studies of infectivity. Additionally, no sampler was found that worked well over the whole size range of particles (about 10 nm to several μm).

We then moved to reviewing bioanalysis techniques such as PCR, ELISA, LAMP, SPR and holographic microscopy. Many of these techniques have on-chip and off-chip (benchtop) versions. While many of these studies did not use air samples, they were still reviewed here as the techniques could be useful for analysis in air. These tests can effectively detect viruses within minutes, and applications for SARS-CoV-2 detection were highlighted.

Overall, air samplers and microfluidic devices have proven useful for virus detection. They can help curb virus outbreaks, as is being seen with novel tests for COVID-19. These technologies will continue to be developed and used for years to come.

6. Future perspectives

Microfluidic technologies need to be further adapted for combatting

COVID-19 and for use in the post-pandemic period. Specifically, rapid air monitoring and PoC diagnosis for known and emerging viruses will be needed to detect and control future outbreaks in their early stages. Devices should be created that operate fully automatically and can transmit information across long ranges. Research in multiplex devices, which can detect multiple viruses at once, will continue to expand.

A limitation of many current devices is that sampling and analysis are usually performed as two separate steps, and the liquid sample collected from air often must be manually put into the chip for analysis. This could highly limit applicability in remote settings because a trained end user is required. To further increase automation, more microfluidic devices that directly use air for analysis (perhaps through a vacuum pump) could be developed and tested. As multiple viruses (including SARS-CoV-2 and influenza) should be monitored for public health protection while a limited number of devices can realistically be produced, spatial and spectral multiplexing capability of these devices must be improved. To create and deploy monitoring and diagnostic devices, it is important for them to be tested in the type of environments where they will ultimately be used, like in office buildings or parks. A controlled laboratory environment is not fully representative of real-world conditions, so future experiments need to emphasize indoor and outdoor field testing. The reusability and durability of devices, and reproducibility among devices of the same design, also needs to be investigated in studies, as they may be used continuously for several months or years.

COVID-19 has had profound economic and social consequences and a second pandemic could be even more devastating. Therefore, more effort must be placed on rapidly identifying novel pathogens and curbing outbreaks. Microfluidic air monitors need to become integrated with next generation sequencing (NGS) to accomplish this. Multiplexing can allow concurrent monitoring for new and existing pathogens, and public health agencies could be alerted when a novel pathogen is identified. Overall, the use of microfluidic air monitoring devices could help manage existing disease outbreaks and prevent new ones.

Declaration of Competing Interest

The authors declare that they have no known competing financial interests or personal relationships that could have appeared to influence the work reported in this paper.

Acknowledgement

The authors would like to thank the Natural Sciences and Engineering Research Council of Canada (NSERC) for financial support provided to PR.

References

[1] S.A. Hassan, F.N. Sheikh, S. Jamal, J.K. Ezeh, A. Akhtar, Coronavirus (COVID-19): a review of clinical features, diagnosis, and treatment, Cureus 12 (2020), https://doi.org/10.7759/cureus.7355.

[2] COVID-19 Map - Johns Hopkins Coronavirus Resource Center [WWW Document], n.d. URL https://coronavirus.jhu.edu/map.html (accessed June 22, 2021).

[3] M. Adnan Shereen, S. Khan, A. Kazmi, N. Bashir, R. Siddique, COVID-19 infection: origin, transmission, and characteristics of human coronaviruses, J. Adv. Res. 24 (2020) 91–98, https://doi.org/10.1016/j.jare.2020.03.005.

[4] N.M. Wilson, A. Norton, F.P. Young, D.W. Collins, Airborne transmission of severe acute respiratory syndrome coronavirus-2 to healthcare workers: a narrative review, Anaesthesia 75 (2020) 1086–1095, https://doi.org/10.1111/anae.15093.

[5] B. Ather, T. Mirza, P.F. Edemekong, Airborne Precautions, StatPearls Publishing, StatPearls Publishing, Treasure Island, FL, 2021.

[6] B.J. Cowling, D.K.M. Ip, V.J. Fang, P. Suntarattiwong, S.J. Olsen, J. Levy, T. M. Uyeki, G.M. Leung, J.S. Malik Peiris, T. Chotpitayasunondh, H. Nishiura, J. Mark Simmerman, Aerosol transmission is an important mode of influenza A virus spread, Nat. Commun. 4 (2013) 1935, https://doi.org/10.1038/ncomms2922.

[7] G. Pardon, L. Ladhani, N. Sandström, M. Ettori, G. Lobov, W. Van Der Wijngaart, Aerosol sampling using an electrostatic precipitator integrated with a microfluidic interface, Sensors Actuators, B Chem. 212 (2015) 344–352, https://doi.org/10.1016/j.snb.2015.02.008.

[8] M. Tan, F. Shen, M. Yao, T. Zhu, Development of an automated electrostatic sampler (AES) for bioaerosol detection, Aerosol Sci. Technol. 45 (2011) 1154–1160, https://doi.org/10.1080/02786826.2011.582193.

[9] J.W. Park, H.R. Kim, J. Hwang, Continuous and real-time bioaerosol monitoring by combined aerosol-to-hydrosol sampling and ATP bioluminescence assay, Anal. Chim. Acta 941 (2016) 101–107, https://doi.org/10.1016/j.aca.2016.08.039.

[10] H.J. Kwon, C.F. Fronczek, S.V. Angus, A.M. Nicolini, J.Y. Yoon, Rapid and sensitive detection of H1N1/2009 virus from aerosol samples with a microfluidic immunosensor, J. Lab. Autom. 19 (2014) 322–331, https://doi.org/10.1177/2211068213504205.

[11] C.D. Chin, V. Linder, S.K. Sia, Lab-on-a-chip devices for global health: past studies and future opportunities, Lab Chip 7 (2007) 41–57, https://doi.org/10.1039/b611455e.

[12] R. Wang, R. Zhao, Y. Li, W. Kong, X. Guo, Y. Yang, F. Wu, W. Liu, H. Song, R. Hao, Rapid detection of multiple respiratory viruses based on microfluidic isothermal amplification and a real-time colorimetric method, Lab Chip 18 (2018) 3507–3515, https://doi.org/10.1039/c8lc00841h.

[13] Y. Song, Microfluidics: Fundamentals, Devices, and Applications, Wiley-VCH, 2018.

[14] B. Nasseri, N. Soleimani, N. Rabiee, A. Kalbasi, M. Karimi, M.R. Hamblin, Point-of-care microfluidic devices for pathogen detection, Biosens. Bioelectron. 117 (2018) 112–128, https://doi.org/10.1016/j.bios.2018.05.050.

[15] J. Mairhofer, K. Roppert, P. Ertl, Microfluidic systems for pathogen sensing: a review, Sensors (Switzerland) 9 (2009) 4804–4823, https://doi.org/10.3390/s90604804.

[16] S.K. Bhardwaj, N. Bhardwaj, V. Kumar, D. Bhatt, A. Azzouz, J. Bhaumik, K. H. Kim, A. Deep, Recent progress in nanomaterial-based sensing of airborne viral and bacterial pathogens, Environ. Int. 146 (2021), 106183, https://doi.org/10.1016/j.envint.2020.106183.

[17] P. Nath, A. Kabir, S.K. Doust, Z.J. Kreais, A. Ray, Detection of bacterial and viral pathogens using photonic point-of-care devices, Diagnostics 10 (2020) 1–24, https://doi.org/10.3390/diagnostics10100841.

[18] J. Zhuang, J. Yin, S. Lv, B. Wang, Y. Mu, Advanced "lab-on-a-chip" to detect viruses – current challenges and future perspectives, Biosens. Bioelectron. 163 (2020), 112291, https://doi.org/10.1016/j.bios.2020.112291.

[19] S. Herfst, M. Böhringer, B. Karo, P. Lawrence, N.S. Lewis, M.J. Mina, C.J. Russell, J. Steel, R.L. de Swart, C. Menge, Drivers of airborne human-to-human pathogen transmission, Curr. Opin. Virol. 22 (2017) 22–29, https://doi.org/10.1016/j.coviro.2016.11.006.

[20] L. Morawska, G.R. Johnson, Z.D. Ristovski, M. Hargreaves, K. Mengersen, S. Corbett, C.Y.H. Chao, Y. Li, D. Katoshevski, Size distribution and sites of origin of droplets expelled from the human respiratory tract during expiratory activities, J. Aerosol Sci. 40 (2009) 256–269, https://doi.org/10.1016/j.jaerosci.2008.11.002.

[21] X. Xie, Y. Li, H. Sun, L. Liu, Exhaled droplets due to talking and coughing, J. R. Soc. Interface 6 (2009) S703–S714, https://doi.org/10.1098/rsif.2009.0388.focus.

[22] H. Holmgren, E. Ljungström, A.-C. Almstrand, B. Bake, A.-C. Olin, Size distribution of exhaled particles in the range from 0.01 to 2.0Mm, J. Aerosol Sci. 41 (2010) 439–446, https://doi.org/10.1016/j.jaerosci.2010.02.011.

[23] J. Gralton, E. Tovey, M.L. McLaws, W.D. Rawlinson, The role of particle size in aerosolised pathogen transmission: a review, J. Infect. 62 (2011) 1–13, https://doi.org/10.1016/j.jinf.2010.11.010.

[24] B. Killingley, J. Nguyen-Van-Tam, Routes of influenza transmission, Influenza Other Respi. Viruses 7 (2013) 42–51, https://doi.org/10.1111/irv.12080.

[25] N95 Respirators, Surgical Masks, and Face Masks | FDA [WWW Document], n.d. URL https://www.fda.gov/medical-devices/personal-protective-equipment-infection-control/n95-respirators-surgical-masks-and-face-masks (accessed July 21, 2020).

[26] J.P. Duguid, The size and the duration of air-carriage of respiratory droplets and droplet-nuclei, J. Hyg. (Lond). 44 (1946) 471–479, https://doi.org/10.1017/S0022172400019288.

[27] J. Ma, X. Qi, H. Chen, X. Li, Z. Zhang, H. Wang, L. Sun, L. Zhang, J. Guo, L. Morawska, S.A. Grinshpun, P. Biswas, R.C. Flagan, M. Yao, COVID-19 patients in earlier stages exhaled millions of SARS-CoV-2 per hour, Clin. Infect. Dis. (2020) ciaa1283, https://doi.org/10.1093/cid/ciaa1283.

[28] M. Small, C.K. Tse, D.M. Walker, Super-spreaders and the rate of transmission of the SARS virus, Phys. D Nonlinear Phenom. 215 (2006) 146–158, https://doi.org/10.1016/j.physd.2006.01.021.

[29] L.M. Casanova, S. Jeon, W.A. Rutala, D.J. Weber, M.D. Sobsey, Effects of air temperature and relative humidity on coronavirus survival on surfaces, Appl. Environ. Microbiol. 76 (2010) 2712–2717, https://doi.org/10.1128/AEM.02291-09.

[30] S. Niazi, R. Groth, L. Cravigan, C. He, J.W. Tang, K. Spann, G.R. Johnson, Susceptibility of an airborne common cold virus to relative humidity, Environ. Sci. Technol. (2021), https://doi.org/10.1021/acs.est.0c06197.

[31] V.A. Mouchtouri, M. Koureas, M. Kyritsi, A. Vontas, L. Kourentis, S. Sapounas, G. Rigakos, E. Petinaki, S. Tsiodras, C. Hadjichristodoulou, Environmental contamination of SARS-CoV-2 on surfaces, air-conditioner and ventilation systems, Int. J. Hyg. Environ. Health 230 (2020), 113599, https://doi.org/10.1016/j.ijheh.2020.113599.

[32] K. Razzini, M. Castrica, L. Menchetti, L. Maggi, L. Negroni, N.V. Orfeo, A. Pizzoccheri, M. Stocco, S. Muttini, C.M. Balzaretti, SARS-CoV-2 RNA detection in the air and on surfaces in the COVID-19 ward of a hospital in Milan, Italy. Sci.

Total Environ. 742 (2020), 140540, https://doi.org/10.1016/j.scitotenv.2020.140540.
[33] M.A. Lane, E.A. Brownsword, J.S. Morgan, A. Babiker, S.A. Vanairsdale, G. M. Lyon, A.K. Mehta, J.M. Ingersoll, W.G. Lindsley, C.S. Kraft, Bioaerosol sampling of a ventilated patient with COVID-19, Am. J. Infect. Control 48 (2020) 1540–1542, https://doi.org/10.1016/j.ajic.2020.07.033.
[34] S. Yezli, J.A. Otter, Minimum infective dose of the major human respiratory and enteric viruses transmitted through food and the environment, Food Environ. Virol. 3 (2011) 1–30, https://doi.org/10.1007/s12560-011-9056-7.
[35] J. Louten, Essential Human Virology, Academic Press Inc, 2016, https://doi.org/10.1016/C2013-0-19118-0.
[36] H. Lodish, D. Baltimore, A. Berk, Viruses: structure, function and uses. Molecular Cell Biology, WH Freeman & Co, New York, 2000.
[37] T. Ji, Z. Liu, G.Q. Wang, X. Guo, S. Akbar khan, C. Lai, H. Chen, S. Huang, S. Xia, B. Chen, H. Jia, Y. Chen, Q. Zhou, Detection of COVID-19: a review of the current literature and future perspectives, Biosens. Bioelectron. 166 (2020), 112455, https://doi.org/10.1016/j.bios.2020.112455.
[38] A. Kenarkoohi, Z. Noorimotlagh, S. Falahi, A. Amarloei, S.A. Mirzaee, I. Pakzad, E. Bastani, Hospital indoor air quality monitoring for the detection of SARS-CoV-2 (COVID-19) virus, Sci. Total Environ. 748 (2020), 141324, https://doi.org/10.1016/j.scitotenv.2020.141324.
[39] H. Nishiura, T. Kobayashi, T. Miyama, A. Suzuki, Smok Jung, K. Hayashi, R. Kinoshita, Y. Yang, B. Yuan, A.R. Akhmetzhanov, N.M. Linton, Estimation of the asymptomatic ratio of novel coronavirus infections (COVID-19), Int. J. Infect. Dis. 94 (2020) 154–155, https://doi.org/10.1016/j.ijid.2020.03.020.
[40] M. Pan, J.A. Lednicky, C.Y. Wu, Collection, particle sizing and detection of airborne viruses, J. Appl. Microbiol. 127 (2019) 1596–1611, https://doi.org/10.1111/jam.14278.
[41] D. Verreault, S. Moineau, C. Duchaine, Methods for sampling of airborne viruses, Microbiol. Mol. Biol. Rev. 72 (2008) 413–444, https://doi.org/10.1128/mmbr.00002-08.
[42] J. Li, A. Leavey, Y. Wang, C. O'neil, M.A. Wallace, C.-A.D. Burnham, A. Cm Boon, H. Babcock, P. Biswas, Comparing the performance of 3 bioaerosol samplers for influenza virus, J. Aerosol Sci. 115 (2018) 133–145, https://doi.org/10.1016/j.jaerosci.2017.08.007.
[43] I. Mirzaee, M. Song, M. Charmchi, H. Sun, A microfluidics-based on-chip impinger for airborne particle collection, Lab Chip 16 (2016) 2254–2264, https://doi.org/10.1039/c6lc00040a.
[44] A.C. Springorum, M. Clauß, J. Hartung, A temperature-controlled AGI-30 impinger for sampling of bioaerosols, Aerosol Sci. Technol. 45 (2011) 1231–1239, https://doi.org/10.1080/02786826.2011.588275.
[45] BioSampler [WWW Document], n.d. URL https://www.skcltd.com/products2/bioaerosol-sampling/biosampler.html#specifications (accessed August 24, 2020).
[46] L. Riemenschneider, M.H. Woo, C.Y. Wu, D. Lundgren, J. Wander, J.H. Lee, H. W. Li, B. Heimbuch, Characterization of reaerosolization from impingers in an effort to improve airborne virus sampling, J. Appl. Microbiol. 108 (2010) 315–324, https://doi.org/10.1111/j.1365-2672.2009.04425.x.
[47] S.A. Grinshpun, K. Willeke, V. Ulevicius, A. Juozaitis, S. Terzieva, J. Donnelly, G. N. Stelma, K.P. Brenner, Effect of Impaction, bounce and reaerosolization on the collection efficiency of impingers, Aerosol Sci. Technol. 26 (1997) 326–342, https://doi.org/10.1080/02786829708965434.
[48] S.C. Hong, J.S. Kang, J.E. Lee, S.S. Kim, J.H. Jung, Continuous aerosol size separator using inertial microfluidics and its application to airborne bacteria and viruses, Lab Chip 15 (2015) 1889–1897, https://doi.org/10.1039/c5lc00079c.
[49] S. Faridi, S. Niazi, K. Sadeghi, K. Naddafi, J. Yavarian, M. Shamsipour, N. Zahra, S. Jandaghi, K. Sadeghniiat, R. Nabizadeh, M. Yunesian, F. Momeniha, A. Mokamel, M.S. Hassanvand, T. Mokhtariazad, A field indoor air measurement of SARS-CoV-2 in the patient rooms of the largest hospital in Iran, Sci. Total Environ. 725 (2020), 138401, https://doi.org/10.1016/j.scitotenv.2020.138401.
[50] A.A. Andersen, New sampler for the collection, sizing, and enumeration of viable airborne particles, J. Bacteriol. 76 (1958) 471–484, https://doi.org/10.1128/JB.76.5.471-484.1958.
[51] J. Appert, P.C. Raynor, M. Abin, Y. Chander, H. Guarino, S.M. Goyal, Z. Zuo, S. Ge, T.H. Kuehn, Influence of suspending liquid, impactor type, and substrate on size-selective sampling of MS2 and adenovirus aerosols, Aerosol Sci. Technol. 46 (2012) 249–257, https://doi.org/10.1080/02786826.2011.619224.
[52] Y.S. Cho, S.-C. Hong, J. Choi, J. Hee, Development of an automated wet-cyclone system for rapid, continuous and enriched bioaerosol sampling and its application to real-time detection, Sensors Actuators B Chem. 284 (2019) 525–533, https://doi.org/10.1016/j.snb.2018.12.155.
[53] D.A. Orsini, K. Rhoads, K. McElhoney, E. Schick, D. Koehler, O. Hogrefe, A water cyclone to preserve insoluble aerosols in liquid flow - an interface to flow cytometry to detect airborne nucleic acid, Aerosol Sci. Technol. 42 (2008) 343–356, https://doi.org/10.1080/02786820802072881.
[54] N. Sandström, T. Frisk, G. Stemme, W. Van Der Wijngaart, Electrohydrodynamic enhanced transport and trapping of airborne particles to a microfluidic air-liquid interface, Proc. IEEE Int. Conf. Micro Electro Mech. Syst. (2008) 595–598, https://doi.org/10.1109/MEMSYS.2008.4443726.
[55] T.G. Foat, W.J. Sellors, M.D. Walker, P.A. Rachwal, J.W. Jones, D.D. Despeyroux, L. Coudron, I. Munro, D.K. McCluskey, C.K.L. Tan, M.C. Tracey, A prototype personal aerosol sampler based on electrostatic precipitation and electrowetting-on-dielectric actuation of droplets, J. Aerosol Sci. 95 (2016) 43–53, https://doi.org/10.1016/j.jaerosci.2016.01.007.
[56] J. Bhardwaj, M.-W.W. Kim, J. Jang, Rapid airborne influenza virus quantification using an antibody-based electrochemical paper sensor and electrostatic particle concentrator, Environ. Sci. Technol. 54 (2020) 10700–10712, https://doi.org/10.1021/acs.est.0c00441.
[57] S.V. Hering, M.R. Stolzenburg, F.R. Quant, D.R. Oberreit, P.B. Keady, A laminar-flow, water-based condensation particle counter (WCPC), Aerosol Sci. Technol. 39 (2005) 659–672, https://doi.org/10.1080/02786820500182123.
[58] S.V. Hering, M.R. Stolzenburg, A method for particle size amplification by water condensation in a laminar, thermally diffusive flow, Aerosol Sci. Technol. 39 (2005) 428–436, https://doi.org/10.1080/027868290953416.
[59] S.V. Hering, S.R. Spielman, G.S. Lewis, Moderated, water-based, condensational particle growth in a laminar flow, Aerosol Sci. Technol. 48 (2014) 401–408, https://doi.org/10.1080/02786826.2014.881460.
[60] I.V. Novosselov, R.A. Gorder, J.A. Van Amberg, P.C. Ariessohn, Design and performance of a low-cost micro-channel aerosol collector, Aerosol Sci. Technol. 48 (2014) 822–830, https://doi.org/10.1080/02786826.2014.932895.
[61] B. Damit, Droplet-based microfluidics detector for bioaerosol detection, Aerosol Sci. Technol. 51 (2017) 488–500, https://doi.org/10.1080/02786826.2016.1275515.
[62] R.M. Hnasko, A. Lin, S. Bagchi, L. Faget, D. Boassa, R.S. Matson, K. Sahagian, ELISA: methods and protocols. Methods in Molecular Biology, Humana Press Inc, 2015, https://doi.org/10.1007/978-1-4939-2742-5_1.
[63] Y. Liu, Y. Tan, Q. Fu, M. Lin, J. He, S. He, M. Yang, S. Chen, J. Zhou, Reciprocating-flowing on-a-chip enables ultra-fast immunobinding for multiplexed rapid ELISA detection of SARS-CoV-2 antibody, Biosens. Bioelectron. 176 (2021), 112920, https://doi.org/10.1016/j.bios.2020.112920.
[64] N. Dimov, M.B. McDonnell, I. Munro, D.K. McCluskey, I.D. Johnston, C.K.L. Tan, L. Coudron, Electrowetting-based digital microfluidics platform for automated enzyme-linked immunosorbent assay, J. Vis. Exp. 156 (2020), e60489, https://doi.org/10.3791/60489.
[65] N. Yanagisawa, D. Dutta, Kinetic ELISA in microfluidic channels, Biosensors 1 (2011) 58–69, https://doi.org/10.3390/bios1020058.
[66] N. Boonham, J. Kreuze, S. Winter, R. van der Vlugt, J. Bergervoet, J. Tomlinson, R. Mumford, Methods in virus diagnostics: from ELISA to next generation sequencing, Virus Res. 186 (2014) 20–31, https://doi.org/10.1016/j.virusres.2013.12.007.
[67] P.-H. Lu, Y.-D. Ma, C.-Y. Fu, G.-B. Lee, A structure-free digital microfluidic platform for detection of influenza a virus by using magnetic beads and electromagnetic forces, Lab on a Chip 20 (2020) 789–797, https://doi.org/10.1039/c9lc01126a.
[68] C. Coarsey, B. Coleman, M.A. Kabir, M. Sher, W. Asghar, Development of a flow-free magnetic actuation platform for an automated microfluidic ELISA, RSC Adv. 9 (2019) 8159–8168, https://doi.org/10.1039/c8ra07607c.
[69] R.B.M. Schasfoort, Introduction to surface plasmon resonance, in: R.B. M. Schasfoort (Ed.), Handbook of Surface Plasmon Resonance, 2017, pp. 1–26, https://doi.org/10.1039/9781788010283-00001.
[70] Y.-F. Chang, W.-H. Wang, Y.-W. Hong, R.-Y. Yuan, K.-H. Chen, Y.-W. Huang, P.-L. Lu, Y.-H. Chen, Y.-M.A. Chen, L.-C. Su, S.-F. Wang, Simple strategy for rapid and sensitive detection of avian influenza a H7N9 virus based on intensity-modulated SPR biosensor and new generated antibody, Anal. Chem. 90 (2018) 1861–1869, https://doi.org/10.1021/acs.analchem.7b03934.
[71] E.V. Usachev, O.V. Usacheva, I.E. Agranovski, Surface plasmon resonance-based real-time bioaerosol detection, J. Appl. Microbiol. 115 (2013) 766–773, https://doi.org/10.1111/jam.12267.
[72] I.E. Agranovski, V. Agranovski, S.A. Grinshpun, T. Reponen, K. Willeke, Collection of airborne microorganisms into liquid by bubbling through porous medium, Aerosol Sci. Technol. 36 (2002) 502–509, https://doi.org/10.1080/02786820753571322.
[73] L. Huang, L. Ding, J. Zhou, S. Chen, F. Chen, C. Zhao, One-step rapid quantification of SARS-CoV-2 virus particles via low-cost nanoplasmonic sensors in generic microplate reader and point-of-care device, Biosens. Bioelectron. 171 (2021), 112685, https://doi.org/10.1016/j.bios.2020.112685.
[74] T. Nicol, C. Lefeuvre, O. Serri, A. Pivert, F. Joubaud, V. Dubée, A. Kouatchet, A. Ducancelle, F. Lunel-Fabiani, H. Le Guillou-Guillemette, Assessment of SARS-CoV-2 serological tests for the diagnosis of COVID-19 through the evaluation of three immunoassays: Two automated immunoassays (Euroimmun and Abbott) and one rapid lateral flow immunoassay (NG Biotech), J. Clin. Virol. 129 (2020), 104511, https://doi.org/10.1016/j.jcv.2020.104511.
[75] L. Zhao, L. Sun, X. Chu, Chemiluminescence immunoassay, TrAC - Trends Anal. Chem. 28 (2009) 404–415, https://doi.org/10.1016/j.trac.2008.12.006.
[76] B. O'farrell, Evolution in lateral flow-based immunoassay systems, in: R. Wong, H. Tse (Eds.), Evolution in Lateral Flow-Based Immunoassay Systems, Humana Press, 2009, pp. 1–31, https://doi.org/10.1007/978-1-59745-240-3_1.
[77] J.L. Wu, W.P. Tseng, C.H. Lin, T.F. Lee, M.Y. Chung, C.H. Huang, S.Y. Chen, P. R. Hsueh, S.C. Chen, Four point-of-care lateral flow immunoassays for diagnosis of COVID-19 and for assessing dynamics of antibody responses to SARS-CoV-2, J. Infect. 81 (2020) 435–442, https://doi.org/10.1016/j.jinf.2020.06.023.
[78] T. Xiang, Z. Jiang, J. Zheng, C. Lo, H. Tsou, G. Ren, J. Zhang, A. Huang, G. Lai, A novel double antibody sandwich-lateral flow immunoassay for the rapid and simple detection of hepatitis C virus, Int. J. Mol. Med. 30 (2012) 1041–1047, https://doi.org/10.3892/ijmm.2012.1121.
[79] Z. Rong, Q. Wang, N. Sun, X. Jia, K. Wang, R. Xiao, S. Wang, Smartphone-based fluorescent lateral flow immunoassay platform for highly sensitive point-of-care detection of Zika virus nonstructural protein 1, Anal. Chim. Acta 1055 (2019) 140–147, https://doi.org/10.1016/j.aca.2018.12.043.
[80] J. Singh, N. Birbian, S. Sinha, A. Goswami, A critical review on PCR, its types and applications, Int. J. Adv. Res. Biol.Sci 1 (2014) 65–80.

[81] F. Shen, M. Tan, Z. Wang, M. Yao, Z. Xu, Y. Wu, J. Wang, X. Guo, T. Zhu, Integrating silicon nanowire field effect transistor, microfluidics and air sampling techniques for real-time monitoring biological aerosols, Environ. Sci. Technol. 45 (2011) 7473–7480, https://doi.org/10.1021/es1043547.
[82] E.G. Huijskens, R.C. Biesmans, A.G. Buiting, C.C. Obihara, J.W. Rossen, Diagnostic value of respiratory virus detection in symptomatic children using real-time PCR, Virol. J. 9 (2012) 276, https://doi.org/10.1186/1743-422X-9-276.
[83] D.M. Olive, M. Simsek, S. Al-Mufti, Polymerase chain reaction assay for detection of human cytomegalovirus, J. Clin. Microbiol. 27 (1989) 1238–1242, https://doi.org/10.1128/jcm.27.6.1238-1242.1989.
[84] N. Farshidfar, S. Hamedani, The potential role of smartphone-based microfluidic systems for rapid detection of COVID-19 using saliva specimen, Mol. Diagn. Ther. 24 (2020) 371–373, https://doi.org/10.1007/s40291-020-00477-4.
[85] R. Prakash, K. Pabbaraju, S. Wong, A. Wong, R. Tellier, K.V.I.S. Kaler, Multiplex, quantitative, reverse transcription PCR detection of influenza viruses using droplet microfluidic technology, Micromachines 6 (2015) 63–79, https://doi.org/10.3390/mi6010063.
[86] Y.T. Yeh, Y. Tang, A. Sebastian, A. Dasgupta, N. Perea-Lopez, I. Albert, H. Lu, M. Terrones, S.Y. Zheng, Tunable and label-free virus enrichment for ultrasensitive virus detection using carbon nanotube arrays, Sci. Adv. 2 (2016), e1601026, https://doi.org/10.1126/sciadv.1601026.
[87] T. Notomi, H. Okayama, H. Masubichi, T. Yonekawa, K. Watanabe, N. Amino, T. Hase, Loop-mediated isothermal amplification of DNA, Nucleic Acids Res. 28 (2000) e63, https://doi.org/10.1093/nar/28.12.e63.
[88] Y. Liu, B. Lu, Y. Tang, Y. Du, B. Li, Real-time gene analysis based on a portable electrochemical microfluidic system, Electrochem. commun. 111 (2020), 106665, https://doi.org/10.1016/j.elecom.2020.106665.
[89] M. Fujino, N. Yoshida, S. Yamaguchi, N. Hosaka, Y. Ota, T. Notomi, T. Nakayama, A simple method for the detection of measles virus genome by loop-mediated isothermal amplification (LAMP), J. Med. Virol. 76 (2005) 406–413, https://doi.org/10.1002/jmv.20371.
[90] Q. Liu, Y. Zhang, W. Jing, S. Liu, D. Zhang, G. Sui, First airborne pathogen direct analysis system, Analyst 141 (2016) 1637, https://doi.org/10.1039/c5an02367j.
[91] Q. Liu, X. Zhang, X. Li, S. Liu, G. Sui, A semi-quantitative method for point-of-care assessments of specific pathogenic bioaerosols using a portable microfluidics-based device, J. Aerosol Sci. 115 (2018) 173–180, https://doi.org/10.1016/j.jaerosci.2017.10.010.
[92] Q. Liu, X. Zhang, Y. Yao, W. Jing, S. Liu, G. Sui, A novel microfluidic module for rapid detection of airborne and waterborne pathogens, Sensors Actuators, B Chem. 258 (2018) 1138–1145, https://doi.org/10.1016/j.snb.2017.11.113.
[93] B.J. Coelho, B. Veigas, H. Águas, E. Fortunato, R. Martins, P.V. Baptista, R. Igreja, A digital microfluidics platform for loop-mediated isothermal amplification detection, Sensors (Switzerland) 17 (2017) 1–11, https://doi.org/10.3390/s17112616.
[94] F. Sun, A. Ganguli, J. Nguyen, R. Brisbin, K. Shanmugam, D.L. Hirschberg, M. B. Wheeler, R. Bashir, D.M. Nash, B.T. Cunningham, Smartphone-based multiplex 30-minute nucleic acid test of live virus from nasal swab extract, Lab Chip 20 (2020) 1621–1627, https://doi.org/10.1039/d0lc00304b.
[95] A. Ganguli, A. Mostafa, J. Berger, M.Y. Aydin, F. Sun, S.A.S. de Ramirez, E. Valera, B.T. Cunningham, W.P. King, R. Bashir, Rapid isothermal amplification and portable detection system for SARS-CoV-2, Proc. Natl. Acad. Sci. U. S. A. 117 (2020) 22727–22735, https://doi.org/10.1073/PNAS.2014739117.
[96] J. Rodriguez-Manzano, K. Malpartida-Cardenas, N. Moser, I. Pennisi, M. Cavuto, L. Miglietta, A. Moniri, R. Penn, G. Satta, P. Randell, F. Davies, F. Bolt, W. Barclay, A. Holmes, P. Georgiou, Handheld point-of-Care system for rapid detection of SARS-CoV-2 extracted RNA in under 20 min, ACS Cent. Sci. (2021), https://doi.org/10.1021/acscentsci.0c01288.
[97] F. Tian, C. Liu, J. Deng, Z. Han, L. Zhang, Q. Chen, J. Sun, A fully automated centrifugal microfluidic system for sample-to-answer viral nucleic acid testing, Sci. China Chem. 63 (2020) 1496–1508, https://doi.org/10.1007/s11426-020-9800-6.
[98] H. Xiong, X. Ye, Y. Li, L. Wang, J. Zhang, X. Fang, J. Kong, Rapid differential diagnosis of seven human respiratory coronaviruses based on centrifugal microfluidic nucleic acid assay, Anal. Chem. 92 (2020) 14297–14302, https://doi.org/10.1021/acs.analchem.0c03364.
[99] H. Zipper, H. Brunner, J. Bernhagen, F. Vitzthum, Investigations on DNA intercalation and surface binding by SYBR Green I, its structure determination and methodological implications, Nucleic Acids Res. 32 (2004), https://doi.org/10.1093/nar/gnh101.
[100] T. van Helvoort, N. Sankaran, How seeing became knowing: the role of the Electron microscope in shaping the modern definition of viruses, J. Hist. Biol. 52 (2019) 125–160, https://doi.org/10.1007/s10739-018-9530-2.
[101] A. Ray, M.U. Daloglu, J. Ho, A. Torres, E. McLeod, A. Ozcan, Computational sensing of herpes simplex virus using a cost-effective on-chip microscope, Sci. Rep. 7 (2017) 4856, https://doi.org/10.1038/s41598-017-05124-3.
[102] A. Ray, M.A. Khalid, A. Demčenko, M. Daloglu, D. Tseng, J. Reboud, J.M. Cooper, A. Ozcan, Holographic detection of nanoparticles using acoustically actuated nanolenses, Nat. Commun. 11 (2020) 171, https://doi.org/10.1038/s41467-019-13802-1.
[103] Q. Wei, H. Qi, W. Luo, D. Tseng, S.J. Ki, Z. Wan, Z. Gorocs, L.A. Bentolila, T.-T. Wu, R. Sun, A. Ozcan, Fluorescent imaging of single nanoparticles and viruses on a smart phone, ACS Nano 7 (2013) 9147–9155, https://doi.org/10.1021/nn4037706.
[104] K. Ming, J. Kim, M.J. Biondi, A. Syed, K. Chen, A. Lam, M. Ostrowski, A. Rebbapragada, J.J. Feld, W.C.W. Chan, Integrated quantum dot barcode smartphone optical device for wireless multiplexed diagnosis of infected patients, ACS Nano 9 (2015) 3060–3074, https://doi.org/10.1021/nn5072792.
[105] V.I. Kukushkin, N.M. Ivanov, A.A. Novoseltseva, A.S. Gambaryan, I.V. Yaminsky, A.M. Kopylov, E.G. Zavyalova, Highly sensitive detection of influenza virus with SERS aptasensor, PLoS One 14 (2019) 1–14, https://doi.org/10.1371/journal.pone.0216247.
[106] H. Chen, S.G. Park, N. Choi, J.Il Moon, H. Dang, A. Das, S. Lee, D.G. Kim, L. Chen, J. Choo, SERS imaging-based aptasensor for ultrasensitive and reproducible detection of influenza virus A, Biosens. Bioelectron. 167 (2020), 112496, https://doi.org/10.1016/j.bios.2020.112496.
[107] H. Liu, E. Dai, R. Xiao, Z. Zhou, M. Zhang, Z. Bai, Development of a SERS-based lateral flow immunoassay for rapid and ultra-sensitive detection of anti-SARS-CoV-2 IgM/IgG in clinical samples, Sensors Actuators B Chem. 329 (2021), 129196, https://doi.org/10.1016/j.snb.2020.129196.
[108] Chongwen Wang, Chaoguang Wang, X. Wang, K. Wang, Y. Zhu, Z. Rong, W. Wang, R. Xiao, S. Wang, Magnetic SERS strip for sensitive and simultaneous detection of respiratory viruses, ACS Appl. Mater. Interfaces 11 (2019) 19495–19505, https://doi.org/10.1021/acsami.9b03920.
[109] M. Uhm, J.M. Lee, J. Lee, J.H. Lee, S. Choi, B.G. Park, D.M. Kim, S.J. Choi, H. S. Mo, Y.J. Jeong, D.H. Kim, Ultrasensitive electrical detection of hemagglutinin for point-of-care detection of influenza virus based on a CMP-NANA probe and top-down processed silicon nanowire field-effect transistors, Sensors (Switzerland) 19 (2019), https://doi.org/10.3390/s19204502.
[110] F. Shen, J. Wang, Z. Xu, Y. Wu, Q. Chen, X. Li, X. Jie, L. Li, M. Yao, X. Guo, T. Zhu, Rapid flu diagnosis using silicon nanowire sensor, Nano Lett. 12 (2012) 3722–3730, https://doi.org/10.1021/nl301516z.
[111] Y. Cui, Q. Wei, H. Park, C.M. Lieber, Nanowire nanosensors for highly sensitive and selective detection of biological and chemical species, Science 293 (2001) 1289–1292, https://doi.org/10.1126/science.1062711.
[112] A. Poghossian, M. Jablonski, D. Molinnus, C. Wege, M.J. Schöning, Field-effect sensors for virus detection: from Ebola to SARS-CoV-2 and plant viral enhancers, Front. Plant Sci. 11 (2020) 1–14, https://doi.org/10.3389/fpls.2020.598103.
[113] G. Seo, G. Lee, M.J. Kim, S.H. Baek, M. Choi, K.B. Ku, C.S. Lee, S. Jun, D. Park, H. G. Kim, S.J. Kim, J.O. Lee, B.T. Kim, E.C. Park, S. Il Kim, Rapid detection of COVID-19 causative virus (SARS-CoV-2) in human nasopharyngeal swab specimens using field-effect transistor-based biosensor, ACS Nano 14 (2020) 5135–5142, https://doi.org/10.1021/acsnano.0c02823.
[114] G. Seo, G. Lee, M.J. Kim, S.H. Baek, M. Choi, K.B. Ku, C.S. Lee, S. Jun, D. Park, H. G. Kim, S.J. Kim, J.O. Lee, B.T. Kim, E.C. Park, S.Il Kim, Correction: rapid detection of COVID-19 causative virus (SARS-CoV-2) in human nasopharyngeal swab specimens using field-effect transistor-based biosensor (ACS nano (2020) 14:4 (5135-5142) DOI: 10.1021/acsnano.0c02823), ACS Nano 14 (2020) 12257–12258, https://doi.org/10.1021/acsnano.0c06726.
[115] P. Qin, M. Park, K.J. Alfson, M. Tamhankar, R. Carrion, J.L. Patterson, A. Griffiths, Q. He, A. Yildiz, R. Mathies, K. Du, Rapid and fully microfluidic Ebola virus detection with CRISPR-Cas13a, ACS Sens. 4 (2019) 1048–1054, https://doi.org/10.1021/acssensors.9b00239.
[116] O. Mayuramart, P. Nimsamer, S. Rattanaburi, N. Chantaravisoot, K. Khongnomnan, J. Chansaenroj, J. Puenpa, N. Suntronwong, P. Vichaiwattana, Y. Poovorawan, S. Payungporn, Detection of severe acute respiratory syndrome coronavirus 2 and influenza viruses based on CRISPR-Cas12a, Exp. Biol. Med. 246 (2021) 400–405, https://doi.org/10.1177/1535370220963793.